

cc
Bali
21.6.91 ✓

VERIFIED
1983
INL... 4

COMPUTERISED

COMPUTERISED

NATIONAL CHEMICAL LABORATORY
No. T.H. ... 146
Date:
LIBRARY

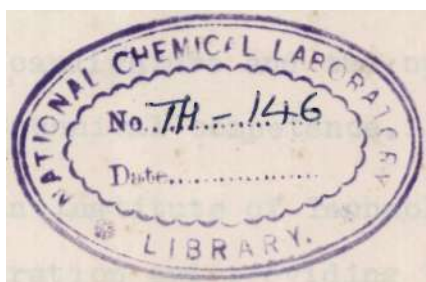
VERIFIED
1981
INL... *[Signature]*

TRANSPORT ACCOMPANIED BY CHEMICAL REACTION IN STAGNATION FLOW

Thesis
Submitted for the degree of

MASTER OF SCIENCE
IN
CHEMICAL ENGINEERING

by
K. S. BALARAMAN



66.023/.028(043)
BAL



DEPARTMENT OF CHEMICAL ENGINEERING
INDIAN INSTITUTE OF TECHNOLOGY
M A D R A S
MAY, 1978.

ACKNOWLEDGEMENT

The author wishes to express his immense gratitude to:

Professor. Dr. M. Satyanarayana and Dr . A. Baradarajan, Department of Chemical Engineering, Indian Institute of Technology, Madras and Dr.L.K.Doraiswamy, Head, Chemical Engineering and Process Development Division, National Chemical Laboratory, Pune for their invaluable guidance and constant encouragement throughout this investigation.

Dr.R.A.Mashelkar, Scientist, National Chemical Laboratory, Pune, for his keen interest, scholarly advice and continued support to this research effort.

Director, National Chemical Laboratory, Pune, for sponsoring the candidature and the opportunity given in improving the technical competence.

Director, Indian Institute of Technology, Madras, for granting registration and providing the necessary facilities during the course work.

Colleagues at the National Chemical Laboratory, Pune, for their encouragement and useful suggestions.

CONTENTS

			<u>PAGE</u>
CHAPTER 1	INTRODUCTION	...	1
	1.1	Introduction	1
	1.2	Phenomenological hetero- geneous catalysis	
	1.3	Object of the work	6
CHAPTER 2	LITERATURE REVIEW	...	7
	2.1	Importance of flow systems in kinetic studies	7
	2.2	Internal flow configurations	11
	2.2.1	Experimental	11
	2.2.2	Analytical	14
	a.	Tubular reactors with laminar flow	14
	b.	Tubular reactors with turbulent flow	14
	2.3	External flow configurations	15
	2.3.1	Flat Plate	15
	2.3.2	Generalized geometry	17
	2.3.3	Sphere	18
	2.3.4	Rotating disc	18
CHAPTER 3	THEORETICAL ANALYSIS	...	20
	3.1	Exact solution of the equation for convective diffusion to the stagnation region of a circular cylinder	20
	3.2	Approximate solutions for $Sc \gg 1$ and $Sc \ll 1$	30

	<u>PAGE</u>
3.3	Solution of the convective diffusion equation with chemical reaction in the stagnation region of a circular cylinder - The method of the 'Uniformly Accessible' surface ... 38
3.4	Characteristic reaction parameters ... 45
CHAPTER 4	DESCRIPTION OF THE APPARATUS 49
4.1	Stagnation region of a circular cylinder - a well defined flow field ... 49
4.2	Description of the apparatus 49
CHAPTER 5	MASS TRANSFER EXPERIMENTS 54
5.1	Purification of Naphthalene 54
5.2	Coating of Naphthalene in the stagnation region ... 54
5.3	Method of analysis ... 55
5.4	Experimental set up and procedure ... 55
CHAPTER 6	KINETIC EXPERIMENTS ... 60
6.1	Deposition of platinum in the stagnation region 60
6.2	Catalyst activity ... 61
6.3	Method of analysis ... 61
6.4	Experimental set up and procedure ... 62
CHAPTER 7	RESULTS AND DISCUSSION ... 66
CHAPTER 8	CONCLUSIONS ... 83

		PAGE
APPENDICIES		
APPENDIX 1	Diffusion coefficient of hydrogen in air and calculation of Schmidt number	85
APPENDIX 2	Mass transfer experiments - Specimen calculation ...	86
APPENDIX 3	Total volume of the reactor	95
APPENDIX 4	Kinetic experiments - Specimen calculation ...	96
REFERENCES	100
NOMENCLATURE	105

LIST OF FIGURES AND TABLES

Figure 3.1	Boundary layer around the circular cylinder	...	20
Figure 3.2	Local Sherwood number as a function of the Schmidt number for flows $U(x)=u_1x^m$...	31
Figure 3.3	Hydrodynamic model of a circular cylinder (in the forward stagnation region) in a flowing stream of reactants	...	39
Figure 3.4	Graphical method for the solution of convective diffusion equation with chemical reaction	...	44
Figure 4.1	Variation of displacement thickness, δ_1 , and momentum thickness, δ_2 with position around the circular cylinder..		50
Figure 4.2	General set up with test section	...	51
Figure 4.3	Test section (enlarged view)..		52
Figure 5.1	Spectrum of naphthalene in rectified spirit at various concentrations at $\lambda = 286$...		56
Figure 5.2	Calibration chart-concentration of naphthalene vs absorbance	...	57
Figure 5.3	Experimental set up for Mass transfer studies	...	58
Figure 6.1	Calibration chart-Hydrogen concentration vs peak height..		63
Figure 6.2	Experimental set up for kinetic studies	...	64
Figure 7.1	Mass transfer around the stagnation region, theory and experiments, $r=0.2 R$...	69

		<u>PAGE</u>
Figure 7.2	Mass transfer around the stagnation region, theory and experiments, $r = 0.3 R$...	70
Figure 7.3	Mass transfer around the stagnation region, theory and experiments, $r = 0.4 R$...	71
Figure 7.4	Concentration of hydrogen in the reactants vs time ...	72
Figure 7.5	First order representation of the reaction with respect to hydrogen ...	74
Figure 7.6	Apparent reaction rate constant K_1 . vs temperature ...	75
Figure 7.7	True reaction rate constant, k vs temperature ...	76
Figure 7.8	Dependence of integrated diffusion (effectiveness) factor, η on the catalytic parameter, C_n ...	80
Figure 7.9	Influence of convective diffusion on the apparent activation energy ...	81
Figure 7.10	Global correction for finite catalyst activity ϕ vs Integrated diffusion (effectiveness) factor ...	81
Table 1	Schmidt number vs function (Schmidt number) ...	32
Table 2	Mass transfer experiments - Results ...	67
Table 3	Kinetic experiments - Results ...	78

CHAPTER 1

INTRODUCTION

1.1. INTRODUCTION

In the last few years, a new and original direction has been developed in chemical kinetics which is aimed at the study of chemical processes in association with the physical processes of heat and material transport. The possibility has arisen out of the unexpected synthesis of such remote fields of science, as chemical kinetics, on the one hand and the theories of heat transfer, diffusion and hydrodynamics on the other. The processes which in classical kinetics were previously regarded as perturbations distorting the progress of a chemical reaction, have acquired special interest in combination with the chemical process. This combination of kinetics with the theory of diffusion, heat transfer and hydrodynamics has enabled us to obtain a number of theoretically valuable results, to develop new methods of measuring reaction rates, and to lay the scientific foundation for the theory of catalytic processes in 'chemical engineering'.

Forced convection systems are frequently used to study the kinetics of fast heterogeneous reactions, since improved rates of reactant transport make it difficult for the active surface to become 'reactant starved' (i.e. induce appreciable local concentration gradients). However, in most cases, the conditions of convective transport are not uniform at all points along a catalytic surface, and for sufficiently active catalysts

(e.g. at sufficiently high surface temperatures), local reactant depletion can cause the apparent (observed) kinetics of the surface reaction to differ drastically from the true kinetics. Thus, although one is usually interested in the true reaction rate constant k the true activation energy E , and the true reaction order n , these parameters will not be obtained as the temperature level and free stream reactant concentration are intentionally changed. Fortunately, however, in many well defined flow systems the magnitude of the falsification is predictable, so that diffusional effects can be removed from kinetic measurements made in the intermediate regime where both chemical kinetics and diffusion govern the observed reaction rates.

1.2. PHENOMENOLOGICAL HETEROGENEOUS CATALYSIS

The term 'heterogeneous' in chemical kinetics refers to reactions occurring at interfaces, i.e. at phase boundaries. The term 'catalysis' implies that the extent of the active surface's participation in the chemical reaction is severely limited since, strictly speaking, the products of a heterogeneously catalyzed reaction cannot include atoms that were originally bound in the lattice of the catalyst itself. Thus, neither the catalyst's bulk properties nor its gross external geometry are changed by virtue of the chemical reaction. Since a catalytic solid cannot initiate a chemical reaction that is thermodynamically impossible, we must,

in general, expect simultaneous chemical change to occur in the fluid or homogeneous phase without the participation of the catalyst. However, it is frequently true that the eligible homogeneous reaction, proceeds at rates that are simply negligible by comparison to the surface reaction. The interface may then be singled out as effectively the site of all of the chemical change in the system, and we therefore look to conditions at the interface as governing the 'velocity' of change. However, observational techniques are insufficiently refined to follow the course of each participating atom or molecule throughout its entire reaction history on the surface. What occurs at this microscopic level must usually be inferred from what can be readily observed, such as the temperature and concentration dependence of the overall reaction rate. Therefore if the relative slowness of reactant transport to the catalyst surface causes the reactant concentrations to be locally depleted, this already difficult task becomes further complicated. To the chemist interested in the interfacial reaction itself, diffusion will seem to be a skilful falsifier and certainly an undesired intruder. For this reason, every attempt is made to carry out experiments on the kinetics of heterogeneous reactions under a set of conditions which relegate diffusion effects to a small or negligible correction. It is then important that we have available both a priori, theoretical criteria for use in the design

of such experiments and simple a posteriori experimental tests for the absence of the effects of external transport phenomena. However, it must not be concluded that kinetic information cannot be obtained in the presence of a simultaneous diffusional limitation. This is quite important, because the extreme in which diffusional transport is sufficiently rapid to play no role in the observed kinetics is not always experimentally accessible, even in forced convection systems. Interpretable kinetic experiments can be carried out in certain well defined flow systems for which the magnitude of the diffusional effect is accurately calculable.

Although the advantages of flow reactors for carrying out catalytic processes on an industrial scale were recognized immediately, the acceptance of flow reactors for carrying out small-scale fundamental kinetic studies has been more gradual. However, current theoretical and practical interest in reactions that are too fast to study by conventional means is inevitably leading to the widespread use of the flow systems in kinetic investigations. These flow systems take diverse forms. However, they may be broken down into two broad categories depending on whether the chemically active fluid/solid interface is moving or at rest in a laboratory coordinate system. In the first class, the solid under investigation may be mechanically rotated in the reactant containing

fluid or may be falling through it for example, under the action of gravity. In the second class, sometimes referred to as fixed catalytic systems, are to be found steady flow reactors (in which the reactant containing fluid flows part or through the catalyst under study) as well as batch reactors where fluid agitation is accomplished by means of some mechanical stirrer. Particularly when transport phenomena cannot be completely avoided, it is important that the investigator understands the fluid mechanics of this system, since in the absence of convective transport information, it will not be possible to extract true kinetic data from such experiments or to generalize the data to apply to different situations.

In the design of experiments one has, therefore, two alternatives. The first consists of attempting to calibrate these transport phenomena by, say, first studying the behaviour of a reaction that is known to be completely diffusion controlled and then bringing these data to bear on an intermediate regime reaction carried out in the same reactor. The second alternative is to obviate the need for an experimental calibration by choosing a class of reactors in which the convective transport situation is well understood theoretically. It would appear that each of these alternatives has merits of its own; however, it will be shown that for non-flow systems a simple calibration procedure previously

implied is, in fact, inadequate, particularly if one is interested in inferring the true kinetic parameters characterizing the reaction. Although the appropriate calibration is within the realm of possibility, its complexity makes this a research project in itself. One is therefore led to adopt a geometry in which this calibration has, in a sense, already been carried out, either theoretically or experimentally.

1.3. OBJECT OF THE WORK

In this work, the attention has been focussed on the important interaction between the hydrodynamics, mass transport and heterogeneous catalytic chemical reaction in a well defined flow field. The kinetics of a diffusionally limited heterogeneous catalytic reaction has been investigated in the stagnation region of a circular cylinder. This geometry was chosen because of the well defined hydrodynamics and because of the fact that the entire stagnation region is equally accessible to the diffusing reactants (uniform accessibility). This characteristic is due to the invariance of the concentration boundary layer thickness (as well as of those for temperature and momentum) with the distance in the stagnation region of a cylinder. The concentration profile and the diffusional flux are thus independent of the position assuming that the catalyst is equally active at all points.

CHAPTER 2

LITERATURE REVIEW

2.1. IMPORTANCE OF FLOW SYSTEMS IN KINETIC STUDIES

Brunner and Nernst (1904) set forth the general theory of reaction velocity in heterogeneous systems. Developing an idea first advanced by Noyes and Whitney (1897) to account for the results of dissolution experiments, Nernst and Brunner postulated that interfacial reactions are fast enough to cause the overall reaction rate to be limited by the rate at which reactants can diffuse across an effectively stagnant film of thickness δ , subsequently called the 'Nernst film' or 'Nernst layer'. The consequences of this postulate were readily deduced and compared with experiments. Three of the most important implications are (1) the apparent kinetics should be first order with respect to bulk reactant concentration, i.e. the rates should depend linearly on this concentration, (2) the temperature dependence of the observed reaction rate should be characteristic of a molecular diffusion process and not that of a chemical reaction and (3) fluid dynamic effects on the rate of reaction, i.e. the effects of agitation, stirring, feed rate, turbulence, etc., should occur by virtue of their effects on the effective diffusion film thickness δ alone.

In discussing this theory, it should be recognized that, as stated, it constituted a qualitative theory, amounting essentially to a dimensional analysis

based on the original postulate, i.e. no means of calculating the effective diffusion layer thickness from first principles was, in fact, suggested. In the years immediately following its formulation, the theory served as the target for a series of critical papers by Centnerszwer (1924), Levich (1942) and Yielstich (1953). Excellent reviews on this material have been given by Levich (1962) and by Bircumshaw and Riddiford (1952). Fundamentally, the critical papers could be divided into two schools. Contributors in the first school accepted the essential Nernst-Brunner idea but were unhappy with the oversimplification of a 'stagnant layer', particularly in the face of evidence on the detailed structure of viscous fluid layers near solid surfaces which was accumulating since the ground-breaking research of Prandtl (1955). On the other hand, those in the second school produced surface reactions that were either paradoxes or that displayed inconsistencies. They suggested that, although the theory was sometimes valid, more often it was not. Conceptually, the second category of objections is more significant since the cornerstone of the Nernst-Brunner theory is the notion of diffusion control; to be dissatisfied only with the notion of stagnant layer is, in fact, merely to be dissatisfied with numerical values. However, the theory was qualitative to begin with, and dimensional analysis cannot

supply absolute values. Therefore, this criticism of the Nernst-Brunner theory led only to more rigorous quantitative formulae for the effective diffusion-layer thickness in particular cases as sighted by Ibl (1963); the 'diffusion-controlled consequences' remained essentially unaltered. On the other hand, the second group displayed a number of important catalytic reactions upon which hydrodynamic factors exerted virtually no influence at all. Temperature coefficients were observed which exceeded anything that could reasonably be attributed to diffusion process alone. Reaction orders not equal to unity were also cited, and even in those cases for which the apparent order was unity, it was cautioned that this by itself did not necessarily confirm the Nernst-Brunner theory, i.e. there are indeed first order surface reactions. Haber (1908) remarked that the Nernst-Brunner theory

teaches us, then, how the rate of diffusion is determining the velocity when other influences are excluded'. He added that the theory 'by no means shows that the chemical velocity must be great as compared with the diffusional velocity but instead, when rightly considered, leaves the point wholly undecided'. Heymann in 1913 was among the first to make a rational attempt at quantitatively reconciling the apparent contradictions just cited. He, as had Haber (1908), Van Name (1916), and others, correctly reasoned that the Nernst-Brunner mechanism must be a limiting case. Heymann's method of generalising the

diffusional theory to include an intrinsic chemical rate was imaginatively exploited and extended to flow systems of practical interest about three decades later by Frank-Kamenetskii (1955). As a result, in the theory of heterogeneous reactions, the so called 'quasi-stationary method' is commonly attributed to him. According to this view, a steady state reactant concentration C_1 is quickly established at the surface such that the rate of diffusional transport to the surface, which is taken to be proportional to the local or instantaneous concentration difference $(C_0 - C_1)$ across the diffusion layer, is identically equal to the chemical rate of conversion at the interface. The latter is, in turn, usually proportional to some power n of the reactant concentration C_1 , where n is the reaction order. The method is extremely simple to use but is seductive in that, when it is applied to flow systems, one is tempted to introduce a coefficient of diffusional transport which has been experimentally or theoretically determined in the absence of surface reaction. Indeed, this is the suggestion of Frank-Kamenetskii (1955). However, for developing flows in which chemical change is occurring in the streamwise direction, the problem of determining the actual local coefficient of diffusional transport is strictly coupled to the kinetics problem. Thus, the error one makes in applying the quasi-stationary method

will depend on chemical kinetic as well as fluid dynamic parameters. Rigorous attacks on this particular problem awaited advances in boundary-layer theory and *were* independently reported by Levich and Meiman (1957), Chambre and Acrivos (1956) and others.

2.2. INTERNAL FLOW CONFIGURATIONS

In the area of diffusion effects on chemical surface reactions, the simplest internal flow system and no doubt the most important from a practical point of view is the tubular reactor. There are many investigations on the internal flow configurations, both analytical and experimental.

2.2.1. Experimental

Baron, Manning and Johnstone(1952) used Damkohler's plug flow analysis to estimate the effect of diffusion on the oxidation of sulfurdioxide in a hollow but porous tube impregnated with vanadium oxide.They found that diffusion resistance significantly increased with temperature but it never exceeded ten per cent. They also assumed that he reactive surface was uniformly accessible, that is pore diffusion was neglected.

Satterfield and Yeung (1963) studied the heterogeneous ecomposition of hydrogen peroxide on platinum and stainless steel in narrow tube in laminar and turbulent

flow. By varying the Reynolds number, they saw the marked effect that diffusion had on the reaction rate. They used the resistance additivity concept to subtract the diffusion effect from the overall rate data. They reported that the approximate analytical solution to the Graetz problem with a first order reaction available to them was highly inaccurate for small conversions. Substantial differences were also found between plug flow and parabolic velocity solutions.

Gidasov and Ellington (1964) reported the results of their study of surface combustion of hydrogen in a vitreous alumina tube coated with platinum. By using high flow rates and making their measurements in the fully developed concentration regime in the centre of the tube, they were able to obtain kinetic data in the temperature range from 200° to 1600° F. Due to interest in the high temperature process, most data were for 600°F and above. At the highest Reynolds number available to them (60,000), the diffusional resistance was small. A correction for whatever resistance remained was not applied due to uncertainties in mass transfer coefficients on eddy diffusivities for mass transfer in the turbulent compressible non-isothermal flow.

Kulacki and Gidaspov (1967) carried out an experimental study of the catalytic combustion of hydrogen air mixtures in a flat rectangular duct flow reactor and with the aid of the measured concentration profiles, it was possible for them to ascertain the reaction rate in the laminar flow regime. Graham and Vidaurri (1968) studied the dehydrogenation of cyclohexane using platinum supported on alumina as catalyst in the temperature range of 470 to 500]°C, pressure range of 21 to 42 atmospheres and Reynolds number range of 20 to 65. A model based on complete external transport control of the overall reaction rate has been proposed, with equilibrium of the fluid at the catalyst surface. Using platinum on silica gel as catalyst at temperature of 150°C, Hencil and Mitschka (1969) calculated the external effectiveness for the hydrogenation of phenol at low Reynolds number (below 0.1). Pignet and Schmidt (1974) have shown that the oxidation of ammonia on Pt-Rh catalyst is very fast requiring contact times of the order of only one m. sec. to accomplish over 95 per cent conversion and considering that the catalyst is used in the form of thin gauze, external mass transfer effects would be expected to be dominant. Horvath et al. (1972) demonstrated that the inner wall of small bore tubes can be coated uniformly with heterogeneous enzyme catalysts and such open tubular reactors retain

their activity for an extended period of time. The reactors of particular interest were those in which the rate of reaction was determined only by the rate of transport of the substrate from the bulk solution to the wall.

2.2.2. Analytical

(a) Tubular reactors with laminar flow

Considerable attention has been devoted to tubular reactors with laminar flow and simple analytical solutions have been reported by Fetting (1962), Hoelscher (1954), Katz (1959), Damkohler (1936), Newman (1931), and Paneth (1931). A lumped parameter approach has been indicated by Mashelkar and Ramachandran (1975).

(b) Tubular reactors, with turbulent flow

Turbulent flow reactors may be of interest for the study of fast interfacial reactions, since the convective diffusion rates are higher. Further, due to the large eddy diffusivities, cross mixing is higher and small radial temperature gradients exist. However, from a theoretical point of view, the turbulent reactor problem is less well defined owing to uncertainties in the velocity profile itself and perhaps more important, in the relation between the eddy diffusivity and the velocity profile. Wissler and Schechter (1962) have carried out calculations for tubular reactors using

the eddy diffusivity function recommended by Sparrow, Hallman and Siegel (1957).

2.3. EXTERNAL FLOW CONFIGURATIONS

It is possible to extract some general conclusions about transfer rates in packed bed flow reactors but formidable mathematical obstacles stand in the way of making accurate predictions of the absolute value of transfer rates. However, there also exists a class of flow systems which are amenable to theoretical attack. Working with such systems also improves our understanding of the transport processes in more complex flow systems.

2.3.1. Flat Plate

Blasius (1960) provided the initial solution to the flow problem. His results were for the case of zero interfacial velocity. In this situation, there is no coupling of mass and momentum transport. For the flat plate geometry the coupling arises in the boundary condition for the wall mass flux. Mickley et al, (1954), in a more detailed theoretical and experimental study, considered the use of blowing or sucking at the plate surface. Concentration and temperature profiles and friction, heat and mass transfer coefficients for various Prandtl or Schmidt numbers were computed.

Friedlander and Litt (1958, 1959) used the flat plate geometry to study mass transfer with chemical reaction. Their model, enabled one to obtain an exact solution to the diffusion and energy equations for a rapid chemical reaction occurring within the laminar boundary layer. In another paper, Friedlander and Litt (1959) examined, in a similar fashion, the distribution of velocity, temperature and concentration near the surface of a burning fuel drop. Friedlander (1962) has also attempted to set the framework for a class of problems associated with chemical change in flowing solutions and has suggested the name 'Hydrodynamic Solution Chemistry'. Again this was based on the simultaneous solution of the conservation equations. Rosner (1963, 1964) has also investigated surface catalyzed reactions on a flat plate with the aim of determining the 'falsification' of reaction order and activation energy. He treated both laminar and turbulent boundary layer examples. The control of the reaction varied with distance down the plate due to the increase of boundary layer thickness. He purposely treated this non-accessible surface to illustrate the changing reaction rate with downstream distance.

2.3.2. Generalized Geometry

Acrivos (1960) has treated the problem of mass transfer with an instantaneous chemical reaction. He generalized the flat plate solution to one of arbitrary surfaces and two dimensional flow using asymptotic solutions which are valid at high Schmidt numbers. Fortunately, for specific geometries such as a flat plate, the assumptions remain valid even for $S_c = 1$. His results reduced to those of Friedlander and Litt for the flat plate.

Asymptotic solutions for mass transfer with large interfacial velocities have also been considered by Acrivos (1960). Again it was for an arbitrary geometry and included the possibility of fluids with variable properties.

Chambre and Acrivos (1956) considered the case of a catalytic surface using a superposition method with boundary layer flow. Their results led to a prediction of surface concentrations. An interesting observation in their results and those of Rosner (1964) is that at the leading edge the rate of reaction is controlled by the free stream concentration since the boundary layer is quite thin and the surface concentration is essentially the free stream value. However, after the boundary layer begins to build up, at some position

66.023 / .028 (043)
BAL

downstream the surface concentration becomes much lower than the free stream value and becomes diffusion limited. This type of behaviour results from the build-up in boundary layer thickness and, hence the local and overall reaction rates are different.

2.3.3. Sphere

Gupalo and Ryazantser (1972) obtained an approximate solution of a steady state problem of mass and heat transfer from a moving solid sphere at small finite Peclet and Reynolds numbers. They considered the case of a first order chemical reaction on the sphere surface.

2.3.4. Rotating disk

Serad (1964) presented an experimental and theoretical study for mass transport with and without chemical reaction on a rotating disk in laminar flow. He developed a model for a rapid, second order irreversible chemical reaction. The rate was expressed in terms of a reaction factor, that is, the rates of transport (in terms of Sherwood numbers) with chemical reaction to that without chemical reaction. The reaction factor was shown to be sensitive to the magnitude of the reactant Schmidt numbers differing from the flat plate results which depend only on their ratio. This was

attributed to the behaviour of the concentration gradients at the disk surface.

Heymach (1969) investigated the kinetics of the hydrogenation of α -methylstyrene on both platinum and palladium catalysts deposited as thin films on a disk which rotated in the liquid hydrocarbon. Recently, White (1972) made an experimental study of diffusion limited heterogeneous catalytic reactions on a rotating disk. He investigated the kinetics of the following hydrogenation reactions; (i) Hydrogenation of α -methylstyrene to cumene over palladium, and (ii) Hydrogenation of phenylacetylene to styrene and subsequent hydrogenation of styrene to ethylbenzene.

CHAPTER 3

THEORETICAL ANALYSIS

3.1. EXACT SOLUTION OF THE EQUATION FOR CONVECTIVE DIFFUSION TO THE STAGNATION REGION OF A CIRCULAR CYLINDER

The theoretical analysis is concerned with methods of calculating mass transfer rates for laminar boundary layer flows when the fluid properties may be considered uniform throughout and internal dissipation of energy is negligible.

The problem of predicting mass transfer rates reduces to the simultaneous solution of (1) the continuity equation (2) the conservation of momentum equation and (3) the conservation of energy equation.

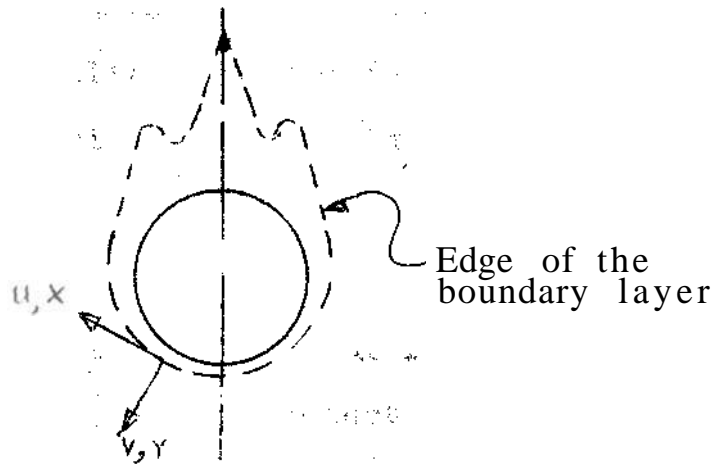


Fig.3.1. Boundary layer around the circular cylinder

Equation of continuity

$$u/x + v/y = 0 \quad (3.1.1)$$

Equation of motion

$$u \frac{du}{dx} + v \frac{dv}{dy} = \frac{1}{\rho} \frac{dp}{dx} + \nu \frac{d^2u}{dy^2} \quad \dots \quad (3.1.2)$$

where,

x = distance measured parallel to the interface from the start of the boundary layer

y = distance measured from the interface and perpendicular to it towards the mainstream

u = velocity component in the x direction

v = velocity component in the y direction

ν = kinematic viscosity of the fluid

ρ = density of the fluid

In the case of potential flow, the equation is simplified still further in that the pressure depends only on x . We shall emphasize this circumstance by writing the derivative as dp/dx so that

$$U \frac{dU}{dX} = -\frac{1}{\rho} \frac{dp}{dx} \quad \dots \quad (3.1.3)$$

Substituting equation (3.1.3) in (3.1.2)

$$u \frac{du}{dx} + v \frac{dv}{dy} = U \frac{dU}{dx} + \nu \frac{d^2u}{dy^2} \quad (3.1.4)$$

where U = value of u in the mainstream.

the boundary conditions being (i) $u = v = 0$ for $y = 0$ and (ii) $u = U$ for $y = \infty$. The equation of continuity is integrated by the introduction of the stream function $\Psi(x, y)$ with

$$u = \frac{\partial \Psi}{\partial y} \quad v = - \frac{\partial \Psi}{\partial x}$$

Thus the equation of motion becomes

$$\frac{\partial}{\partial y} \left(\frac{\partial \Psi}{\partial y} \right)^2 - \frac{\partial}{\partial x} \left(\frac{\partial \Psi}{\partial x} \right)^2 = U \frac{dU}{dx} + \nu \frac{\partial^3 \Psi}{\partial y^3}$$

with the boundary conditions

$$\frac{\partial \Psi}{\partial x} = 0 \quad \text{and} \quad \frac{\partial \Psi}{\partial y} = 0 \quad \text{for} \quad y = 0$$

$$\text{and} \quad \frac{\partial \Psi}{\partial y} = U \quad \text{for} \quad y = \infty$$

er to discuss the question of 'similarity' dimensionless quantities are introduced. All lengths are reduced with the aid of a suitable reference length L , and all velocities are made dimensionless with reference to a suitable velocity U . As a result, the Reynolds number $Re = U L / \nu$ appears in the equation

Simultaneously the y coordinate is referred to the dimensionless scale factor $g(x)$, so that we put

$$\xi = \frac{x}{L}, \quad \eta = \frac{y\sqrt{\text{Re}}}{Lg(x)} \quad \dots (3.1.6)$$

The stream function is made dimensionless by the substitution

$$f(\xi, \eta) = \frac{\psi(x, y)\sqrt{\text{Re}}}{LU(x)g(x)} \quad \dots (3.1.7)$$

Consequently the velocity components become

$$\begin{aligned} u &= \frac{\partial \psi}{\partial y} = U \frac{\partial f}{\partial \eta} = Uf' \\ -\sqrt{\text{Re}} \, v &= \sqrt{\text{Re}} \frac{\partial \psi}{\partial x} \\ &= Lf \frac{d}{dx} (Ug) + Ug \left(\frac{\partial f}{\partial \xi} - \frac{Lg'}{g} \eta f' \right) \end{aligned} \quad (3.1.8)$$

where the prime f' denotes differentiation with respect to η and with respect to x in g' . It is now seen directly from equation (3.1.8) that the velocity profiles $u(x, y)$ are similar in the previously defined sense, when the stream function f depends only on the variable η , equation (3.1.6), so that the dependence of f on x is cancelled. In this case, moreover the partial differential equation for the stream function, equation (3.1.5) must reduce itself to an ordinary differential equation for $f(\eta)$. If we now proceed to investigate the conditions under which the reduction of equation (3.1.5) takes place, we shall obtain the condition which must be satisfied by the potential flow $U(x)$ for such similar solutions to exist.

If we introduce now the dimensionless variables from equations (3.1.6) and (3.1.7) into equation (3.1.5) we obtain the following differential equation for $f(\xi, \eta)$

$$f'''' + \alpha f f'' + \beta(1-f'^2) = \frac{U}{U_\infty} g^2 \left(f' \frac{\partial f'}{\partial \xi} - f'' \frac{df}{d\xi} \right) \quad \dots (3.1.9)$$

where α and β are contractions for the following functions of x

$$\alpha = Lg/U \, d/dx (Ug); \quad \beta = L/U \, g^2 U' \quad \dots (3.1.10)$$

where $U' = dU/dx$. The boundary conditions for equation (3.1.9) are $f = 0$ and $f' = 0$ for $\eta = 0$ and $f' = 1$ for $\eta = \infty$.

To determine from equation (3.1.10) the conditions for $U(x)$ and $g(x)$:

From equation (3.1.10) we obtain

$$2\alpha - \beta = L/U \, d/dx g^2 U$$

and hence if $2\alpha - \beta \neq 0$,

$$U/U \, g^2 = (-2\alpha - \beta) X / L \quad \dots (3.1.11)$$

Further from equation (3.1.10) we have

$$\alpha - \beta = L/U \, g g' U$$

and hence

$$(\alpha - \beta) U'/U = L/U g^{2U} g'/g = \beta g'/g$$

so that upon integration

$$(U/U)^{(\alpha-\beta)} = K g^\beta \dots \quad (3.1.12)$$

where K is a constant. The elimination of g from equations (3.1.11) and (3.1.12) yields the velocity distribution of the potential flow

$$U/U = K^{(2/2\alpha-\beta)} [(2\alpha-\beta)X/L]^{(\beta/2\alpha-\beta)} \dots \quad (3.1.13)$$

$$\text{and } \sqrt{(2\alpha-\beta) \frac{X}{L}} (U/U)^{-1/2} \dots \quad (3.1.14)$$

(It will be recalled that the case $(2\alpha - \beta) = 0$ has been excluded).

As seen from equation (3.1.10) the result is independent of any common factor of α and β , as it can be included in g . Therefore as long as $\alpha \neq 0$, it is permissible to put $\alpha = +1$, without loss of generality. It is furthermore, convenient to introduce a new constant m to replace β by putting

$$m = \beta/2 - \beta \dots \quad (3.1.15)$$

as in this way, the physical meaning of the solution will become clearer. Hence

$$\beta = 2m/m+1$$

so that with $a = 1$, the velocity distribution of the potential flow and the scale factor g for the ordinate become

$$U/U = K^{(1+m)} \left(\frac{2}{1+m}, X/L \right)^m \dots \quad (3.1.16)$$

$$g = \sqrt{\frac{2}{m+1} \frac{x}{L} \frac{U \infty}{U}} \dots \quad (3.1.17)$$

and the transformation equation (3.1.6) for the ordinate is

$$\eta = y \sqrt{\frac{m+1}{2}, \frac{U}{L/x}} \dots \quad (3.1.18)$$

It is thus concluded that similar solutions of the boundary layer equations are obtained when the velocity distribution of the potential flow is proportional to a power of the length of arc, measured along the wall from the stagnation point. Such potential flows occur in the neighbourhood of the stagnation point of a circular cylinder and it is very easy to verify with the aid of potential flow theory that we have

$$U(x) = \frac{m}{u_1 x} \dots \quad (3.1.19)$$

From equation (3.1.18) it follows that the transformation of the independent variable y , which leads to an ordinary differential equation is

$$\eta = y \sqrt{\frac{m+1}{2} \frac{U}{\nu x}} = y \sqrt{\frac{m+1}{2} X^{\frac{m-1}{2}} \frac{U}{\nu}} \quad \dots \quad (3.1.20)$$

The equation of continuity is integrated by the introduction of a stream function for which we put

$$\underline{\Psi}(x,y) = \sqrt{\frac{2}{m+1}} \sqrt{\nu u} \, X^{(m+1/2)} f(\eta)$$

as seen from equations (3.1.7) and (3.1.17)

Thus the velocity components become

$$u = u_1 x^m f'(\eta) = U f'(\eta) \dots (3.1.21)$$

$$\text{or } f'(\eta) = u/U$$

$$v = -\sqrt{\frac{m-1}{2} \frac{U \nu}{x}} \left\{ \eta f'' \right\} \dots (3.1.22)$$

Introducing the values of u and v into the equation of motion, equation (3.1.4) and dividing by $\mu u_1 x^{2m-1}$ and putting as in equation (3.1.15).] $m = \beta/2 - \beta$ and $2m/m+1 = \beta$

we obtain the following differential equation for $f(\eta)$

$$f'''' + ff'' + \beta(1 - f')^2 = 0 \quad (3.1.23)$$

and its boundary conditions are

$$\eta = 0 : f = 0, f' = 0 ; \eta = \infty, f' = 1$$

If the similarity variable η defined in equation (3.1.20) were replaced by the independent variable

$\eta = y \sqrt{U(x)/\nu x}$ the differential equation for the function $f'(\eta) = u/U$ would change its form to

$$f'''' + m+1/2 ff'' + m(1 - f'^2) = 0 \quad \dots \quad (3.1.24)$$

Rate of mass transfer around the stagnation region of the cylinders

Assuming uniform material properties and using rectangular coordinates, the two dimensional convective diffusion equation reduces to

$$u \frac{c}{x} + v \frac{c}{y} = D_c \nabla^2 c \quad \dots \quad (3.1.25)$$

where $D_c =$ Diffusion coefficient

The boundary conditions associated with equation (3.1.25) are: in the mainstream $C = C_0$ and in the fluid at the interface $C = C_1$.

The dimensionless concentration of the form

$$\theta = \frac{C - C_0}{C_1 - C_0}$$

satisfies the equation

$$\theta'' + m+1/2 Sc f \theta' = 0 \quad \dots \quad (3.1.26)$$

with boundary conditions

$$\eta = 0, \theta = 1 \text{ and } \eta \rightarrow \infty, \theta = 0$$

The local Sherwood number Sh_x is given by the equation:

$$(2-\beta)^{\frac{1}{2}} \frac{Sh_x}{\sqrt{Re_x}} = F(m, Sc) = \left\{ \int_0^{\infty} \exp[-Sc \sqrt{\frac{m+1}{2}} \int_0^{\eta} f(\eta) d\eta] d\eta \right\}^{-1} \quad (3.1.27)$$

In the neighbourhood of a stagnation region, where the velocity distribution is represented by $U(x) = u_1 x^m$, we have $m = 1$, $\beta = 1$. The Sherwood number for mass transfer defined in equation (3.1.26) can be represented by the equation

$$\frac{Sh_x}{(Re_x)^{\frac{1}{2}}} = F(Sc, 1) = F(sc) = \left[\int_0^{\infty} \exp \left\{ -Sc \int_0^{\eta} f(\eta) \right\} d\eta \right]^{-1} \quad (3.1.28)$$

For a circular cylinder we put $U(x) = 2 U \sin(x/r)$ so that $u_1 = 4 U = \nu / D$. Hence

$$\begin{aligned} \frac{Sh_x}{(Re_x)^{\frac{1}{2}}} &= \frac{k_g \cdot x}{D_c} \sqrt{\frac{D \nu}{4 U \infty x^2}} \\ &= (1/2) \frac{k_g D}{D_c} \sqrt{\frac{\nu}{4 U \infty D}} \end{aligned}$$

$$Sh_x / (Re_x)^{1/2} = (1/2) Sh_D / (Re_D)^{1/2} = F(Sc)$$

$$\frac{1}{2} \frac{Sh_D}{(Re_D)^{\frac{1}{2}}} = \int_0^{\infty} \left[\exp \left\{ -Sc \int_0^{\eta} f(\eta) d\eta \right\} \right]^{-1} = F(Sc) \quad (3.1.29)$$

where

Sh_D = Sherwood number around the cylinder

Re_D = Reynolds number around the cylinder

k_g = Mass transfer coefficient cm/sec.

D_c = Diffusion coefficient cm^2/sec .

$F(Sc)$ = Function of Schmidt number

The integration was done by a computer using the fourth order Runse-Kutta process and the functions

$$f, f', f'', \int_0^{\eta} f d\eta \text{ and } \left[\int_0^{\infty} \exp \left\{ -Sc \int_0^{\eta} f(\eta) d\eta \right\} \right]^{-1}$$

evaluated. The function $F(Sc)$ corresponding to various

[Schlichting (1968)] and the numerical values are given in Table 1.

3.2. APPROXIMATE SOLUTIONS FOR $Sc \gg 1$ and $Sc \ll 1$

The two dimensional convective diffusion equation is

$$u \frac{\partial c}{\partial x} + v \frac{\partial c}{\partial y} = D_c \frac{\partial^2 c}{\partial y^2} \quad \dots(3.2.1)$$

where D_c is the diffusion coefficient

The function $F(Sc)$ in the equation for the calculation of the coefficient of mass transfer in the neighbourhood of a stagnation point, where $n = 1$, $\beta = 1$.

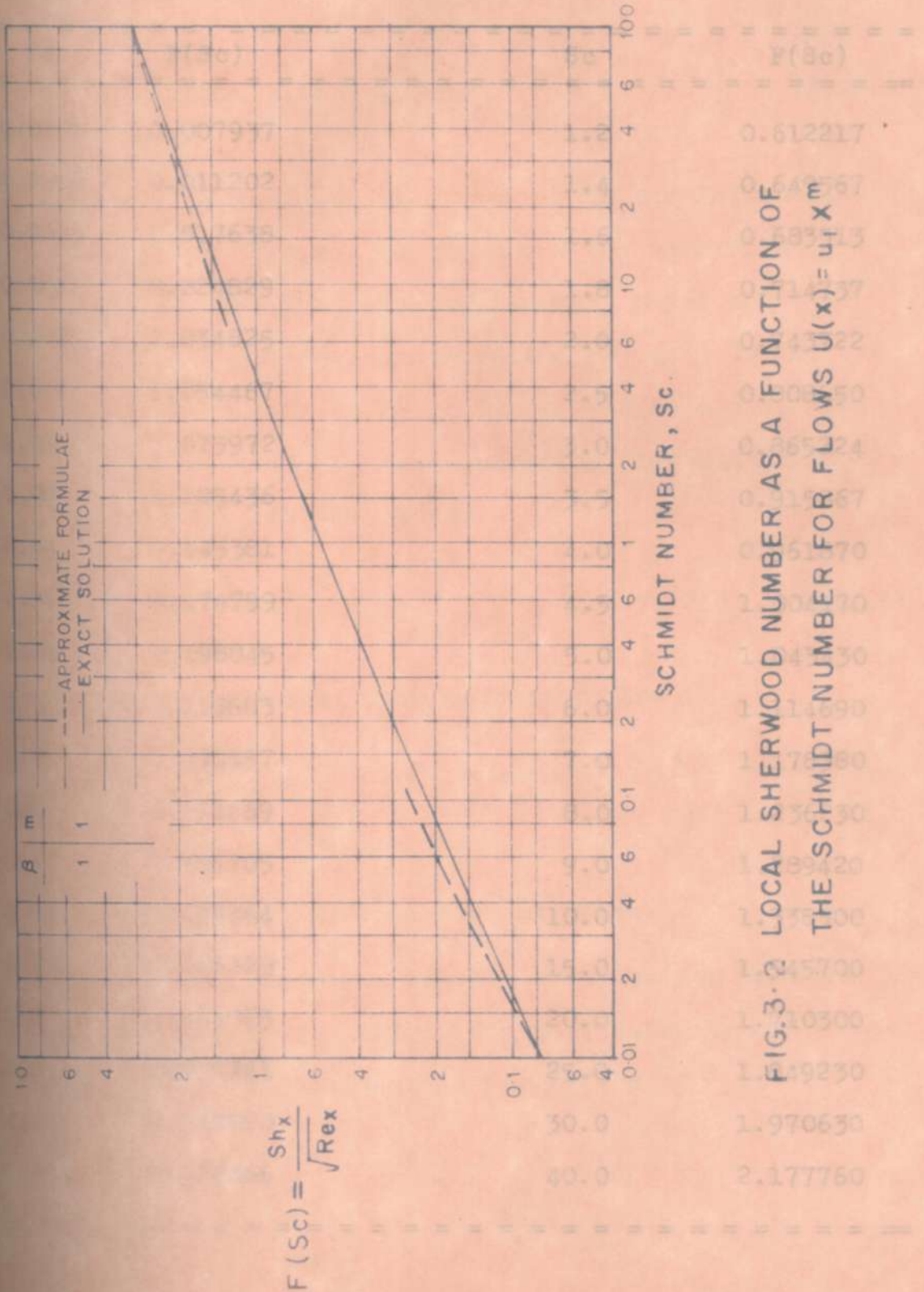


FIG.3-2 LOCAL SHERWOOD NUMBER AS A FUNCTION OF THE SCHMIDT NUMBER FOR FLOWS $U(x) = u_1 x^m$

TABLE 1

The function $F(Sc)$ in the equation for the calculation of the coefficient of mass transfer in the neighbourhood of a stagnation point, where $m = 1$, $\beta = 1$.

Sc	F(Sc)	Sc	F(Sc)
0.0001	0.007937	1.2	0.612217
0.0002	0.011202	1.4	0.649567
0.0005	0.017638	1.6	0.683513
0.001	0.024829	1.8	0.714737
0.002	0.034825	2.0	0.743722
0.005	0.054467	2.5	0.808650
0.01	0.075972	3.0	0.865224
0.02	0.105436	3.5	0.915867
0.04	0.145381	4.0	0.961870
0.06	0.174799	4.5	1.004170
0.08	0.198845	5.0	1.043430
0.1	0.219503	6.0	1.114690
0.2	0.296357	7.0	1.178380
0.3	0.351469	8.0	1.236230
0.4	0.395765	9.0	1.289420
0.5	0.433364	10.0	1.338300
0.6	0.466329	15.0	1.545700
0.7	0.495865	20.0	1.710300
0.8	0.522741	25.0	1.849230
0.9	0.547820	30.0	1.970630
1.0	0.570466	40.0	2.177760

It is possible to integrate equation (3.2.1) from $y = 0$ to $y = \infty$ and to obtain the concentration flux equation

$$\frac{d}{dx} \int_0^{\infty} [u(C - C_0)] dy = -D_c \left(\frac{\partial C}{\partial y} \right)_{y=0} \quad \dots \quad (3.2.2)$$

In order to evaluate the integral on the left hand side of equation (3.2.2), we introduce the variables

$\lambda = y/\delta$ for the velocity boundary layer and

$\lambda_c = y/\delta_c$ for the concentration boundary layer. We

denote further their ratio by $\beta = \delta_c/\delta$ and we assume that the velocity and concentration distributions respectively have the forms:

$$u = U(x) [2\lambda A - 2\lambda^3 + \lambda^4] = U(x) F(\lambda) \quad (3.2.3)$$

where $U(x)$ = Velocity in potential flow

$$\begin{aligned} C - C_0 &= (C_1 - C_0) [1 - 2\lambda_c + 2\lambda_c^3 - \lambda_c^4] \\ &= (C_1 - C_0) L(\lambda_c) \quad \dots \quad (3.2.4) \end{aligned}$$

where C_1 is the surface concentration.

The form of the concentration distribution function is so selected as to ensure identical velocity and concentration distribution for $\delta_c = \delta$.

On substituting equations (3.2.3) and (3.2.4) into (3.2.2) we obtain;

$$d/dx \{ \delta_c U H(\eta) \} = 2 D_c / \delta_c \dots \quad (3.2.5)$$

Here $H(\eta)$ is a universal function of $\eta = \delta_c/\delta$ which turns out to be given by

$$H = \int_0^{\infty} F(\lambda) L(\lambda) d\lambda_c \dots \quad (3.2.6)$$

Performing the indicated integrations, we obtain

$$H(\eta) = 2/15 - 3/140 \eta^3 + 1/180 \eta^4 \text{ for } \eta < 1$$

$$H(\eta) = 3/10 - 3/10 \eta + 2/15 \eta^2 - 3/140 \eta^4$$

for $\eta > 1$

The integration of (3.2.5) yields

$$(\delta_c U H)^2 = 4 D_c \int_0^x U H dx \dots \quad (3.2.7)$$

The velocity boundary layer thickness δ can be evaluated with the aid of equation (10.37) given in Schlichting (1968).

$$\delta^2 = \int_0^x /U^6 U^5 dx \dots (3.2.8)$$

Upon dividing equation (3.2.7) by (3.2.8) we obtain

$$H^2(x) = \frac{4/34 \int_0^x U^4 H dx}{H \int_0^x U^5 dx} \quad (3.2.9)$$

Since $H(x)$ is a known function, the preceding equation can be used to determine $U(x)$. The calculation is best performed by successive approximations, starting with the initial assumption that $U = \text{constant}$.

Hence we obtain

$$H^2(x) = \frac{4/34 \int_0^x U^4 dx}{\int_0^x U^5 dx} \quad (3.2.10)$$

The resulting value of U is now introduced into the left hand side of equation (3.2.9) thus leading to an improved value of U . In general, two steps in the iteration are found to be sufficient.

TWO DIMENSIONAL STAGNATION FLOW

For a circular cylinder $U(x) = 2 U_\infty \sin \theta = 2 U_\infty \sin x/r$

where $U(x)$ = velocity in potential flow

U_∞ = Free stream velocity

x = distance measured along the surface

r = radius of the cylinder

θ = angle around the cylinder measured from the stagnation point

Substituting the expression for U(x) in equation (3.2.11) in equation (3.2.9) gives

$$^2 H(\theta) = \frac{2/17 \int_0^\theta \sin^4 \phi \int_0^\phi H \sin \phi \, d\phi}{\int_0^\theta \sin^5 \phi \, d\phi} \dots \quad (3.2.12)$$

and if H were constant, this would reduce to

$$^2 H(\theta) = \frac{2/17 \int_0^\theta \sin^4 \phi \int_0^\phi \sin \phi \, d\phi}{\int_0^\theta \sin^5 \phi \, d\phi} \dots \quad (3.2.13)$$

First the value of θ at stagnation is desired. The above equation is of the form 0/0 and is therefore indeterminate at $\theta = 0$. Applying L' Hospital's rule and differentiating the numerator and the denominator once the equation was still found to be indeterminate. However, a second differentiation and using

$$\int_0^\theta \sin \phi \, d\phi = 1 - \cos \theta \text{ gives}$$

$$^2 H(\theta) = \frac{2/17 (1 - \cos \theta)}{5 \cos \theta - 2/\cos \theta} = \frac{6/17 (1 - \cos \theta)}{5 \cos \theta - 2/\cos \theta}$$

at $\theta = 0$

...(3.2.14)

The thickness δ is required. Equation (3.2.8) with substitution for $U(x)$ is

$$\delta^2 = \frac{17/2 \int_0^\theta \sin^5 \phi \, d\phi}{\sin^6 \theta} \sqrt{U} \quad \dots \quad (3.2.15)$$

which is indeterminate at $\theta = 0$

Applying L'Hospital rule

$$\delta^2 = D/U \sin^5 \theta / 6 \sin \theta \cos \theta \quad 17/12 DV/U \text{ at } \theta = 0 \quad \dots (3.2.16)$$

$$\text{and } \delta = 1.190 \left(D \sqrt{U} \right)^{1/2} \quad \dots \quad (3.2.17)$$

Hence the Sherwood number Sh_D based on diameter becomes

$$Sh_D = 1.322 (Re_D)^{1/2} (Sc)^{1/3} \text{ FOR } < 1 \text{ or } Sc < 0 \quad \dots (3.2.18)$$

$$Sh_D = 1.596 (Re_D)^{1/2} (Sc)^{1/2} \text{ for } > 1 \text{ or } Sc > 0 \quad \dots (3.2.19)$$

(The local Sherwood number Sh_x is given by the equations

$$Sh_x = 0.661 (Re_x)^{1/2} (Sc)^{1/3} \text{ for } Sc < 0$$

$$Sh_x = 0.798 (Re_x)^{1/2} (Sc)^{1/2} \text{ for } Sc > 0$$

since

$$Sh_x / (Re_x)^{1/2} = 1/2 Sh_D / (Re_D)^{1/2}$$

The approximate solutions are also plotted in Fig. 3.2. As seen from the figure they agree favourably with the exact solutions reported.

3.3. SOLUTION OF THE CONVECTIVE DIFFUSION EQUATION WITH CHEMICAL REACTION IN THE STAGNATION REGION OF A CIRCULAR CYLINDER - THE METHOD OF THE 'UNIFORMLY ACCESSIBLE' SURFACE.

The analysis of the interaction between convective diffusion and chemical reaction in flow reactors usually requires elaborate mathematical treatment. The solution of equations describing an isothermal tubular reactor with catalytically active wall and first order reaction has been obtained by separation of variables [Schmidt (1952)], by integral equations [Chambre and Acrivos (1956)], by inversion of integral equations [Katz (1959)]» and by the quasi-stationary method [Frank-Kamenetskii (1955)]. Korenkov et al. (1974) studied the diffusion boundary layer with n order chemical reaction at the surface. They found the distribution of the concentrations along the surface and also determined the local Nusselt numbers. We propose below a simple relation to express the interaction between the reaction and diffusion.

BASIC ASSUMPTIONS

Let us consider the steady state flow of an incompressible carrier fluid over impermeable catalyst solid as shown in Fig. 3.3. We assume:

Fig.3.3

- (i) The bulk concentration of the reactant present in the carrier fluid is C_0 .
- (ii) Implicit in the diluteness assumption is the property that the fluid is unaffected by reactant diffusion and chemical surface reaction so that the fluid motion is obtainable directly from experiments in the absence of reaction or from an independent study of the equations of overall continuity and motion.

Subject to the above assumptions, the convective diffusion in rectangular coordinates takes the form

$$u \frac{\partial C}{\partial x} + v \frac{\partial C}{\partial y} = D_0 \nabla^2 C \quad \dots (3.3.1)$$

where

- x = distance measured parallel to the surface
- y = distance measured from the surface in the perpendicular direction
- u = velocity component in the x direction
- v = velocity component in the y direction
- D_0 = diffusion coefficient of the reactant
- C = concentration of the reactant

In the forward stagnation region of a cylinder

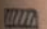
- U = FREE STREAM VELOCITY, u = VELOCITY TANGENTIAL TO THE SURFACE
- v = VELOCITY NORMAL TO THE SURFACE, δ = CONCENTRATION BOUNDARY LAYER THICKNESS
-  CATALYST SURFACE

FIG. 3.3 HYDRODYNAMIC MODEL OF A CIRCULAR CYLINDER (FORWARD STAGNATION REGION) IN A FLOWING STREAM OF REACTANTS

- (i) The bulk concentration of the reactant present in the carrier fluid is C_0 .
- (ii) Implicit in the diluteness assumption is the property that the fluid is unaffected by reactant diffusion and chemical surface reaction so that the fluid motion is obtainable directly from experiments in the absence of reaction or from an independent study of the equations of overall continuity and motion.

Subject to the above assumptions, the convective diffusion equation in rectangular coordinates takes the form

where

- x = distance measured parallel to the surface
 y = distance measured from the surface in the perpendicular direction
 u = velocity component in the x direction
 v = velocity component in the y direction
 D_c = diffusion coefficient of the reactant
 C = concentration of the reactant

In the forward stagnation region of a cylinder the mass transfer coefficient is uniform over the surface. This reduces equation (3.3.1) to

$$v_y(y) \frac{dc}{dy} = (D_c^2 \frac{d^2C}{dy^2}) \dots (3.5.2)$$

This differential equation is easily solved for the entire concentration field $C(y)$ with the boundary conditions

$$(i) \text{ at } y = 0, C = C_1 \dots (3.3/3)$$

$$(ii) \text{ as } y \rightarrow \infty, C = C_0 \dots (3.3.4)$$

where C_1 is the surface concentration and C_0 is the bulk concentration

By integrating (3.3.2) we obtain

$$\frac{dc}{dy} = a_1 \exp\left\{-\frac{1}{D_c} \int_0^y v_y dy\right\} \dots (3.3.5)$$

and by second integration,

$$C = a_1 \int_0^y \exp\left\{-\frac{1}{D_c} \int_0^{\lambda} v_y dy\right\} d\lambda + a_2 \dots (3.3.6)$$

from (3.3.5)

$$\left(\frac{dc}{dy}\right)_{y=0} = a_1 \dots (3.3.7)$$

Applying (3.3.3) in (3.3.6) we get

$$C_1 = a_2 \dots (3.3.8)$$

The flux of species j (equal to the rate of reaction at the surface, R) has the form

$$j = -D_c \left(\frac{dc}{dy}\right)_{y=0} = k_s C_1^n = R \dots (3.3.9)$$

Substituting (3.3.7) and (3.3.8) in (3.3.9) we get

$$j = -D_c a_1 = k_s a_2 = R \dots (3.3.10)$$

where k_s is the true reaction rate constant

Applying b.c.(ii) i.e. (3.3.4) in (3.3.6) we get

$$C_o = \int_0^{\infty} \left\{ \frac{1}{D_c} \int_0^{\lambda} v_y dy' \right\} d\lambda + a_2 \dots (3.3.11)$$

The integral of the equation (3.3.11)

$$\left[\int_0^{\infty} \exp \left\{ \frac{1}{D_c} \int_0^{\lambda} v_y dy' \right\} \right] \text{ gives } \delta_c, \text{ the boundary layer thickness}$$

$$\text{Hence } C_o = a_1 \delta_c + a_2 \dots (3.3.12)$$

$$\text{or } a_1 = -C_o - 2/\Delta_c = C_o - C_1 / \delta_c \dots (3.3.13)$$

Then from equation (3.3.10), we obtain

$$C_1^{n+1} D_c / k_s \delta_c C_1 - D_c C_o / \delta_c = 0 \dots (3.3.14)$$

For first order reaction, i.e. $n = 1$

from (3.3.14), $C_1 = D_c C_o / k_s \delta_c + D_c = C_o / k'_s \delta_c + 1$ or

$$C_1 = C_o / k_s \frac{D_c}{\delta_c} = k_g C_o / k_s + k_g \dots (3.3.15)$$

where $k_g = \text{mass transfer coefficient} = D_c / \delta_c$

$$\text{Rate } jR = k_s C_1 = k_s k_g / k_s k_g C_o = K.C_o \dots (3.3.16)$$

where K is the observed or apparent reaction rate constant

$$\text{Therefore } K = K_s K_g / K_g K_s + K_g \dots (3.3.17)$$

$$\text{or } 1/K = 1 / K_s + 1/ K_g \dots (3.3.18)$$

If the order of reaction, n is not equal to 1, then equation (3.3.14) may be conveniently solved in dimensionless form. By introducing the dimensionless concentration, $= C_1 / C_0$ and the dimensionless parameter $1/\omega = \delta_c K_s / Dc$

equation (3.3.14) may be rewritten as

$$\omega^n = 1 - \dots (3.3.19)$$

This equation is solved graphically as shown in Fig.3.4. In figure 3.4 the straight lines originating from the point $\omega = 1$ and having a slope $1/\omega$ correspond to the right side of the equation (3.3.19). The curves originating from the point $\omega = 0$ represents the left side of the (3.3.19) for various values of n . The points of intersection of the curves and the straight lines correspond to the solution of the equation (3.3.19). At a given n , the different points of intersection correspond to the different values of the parameter

3.4. CHARACTERISTIC REACTION PARAMETERS

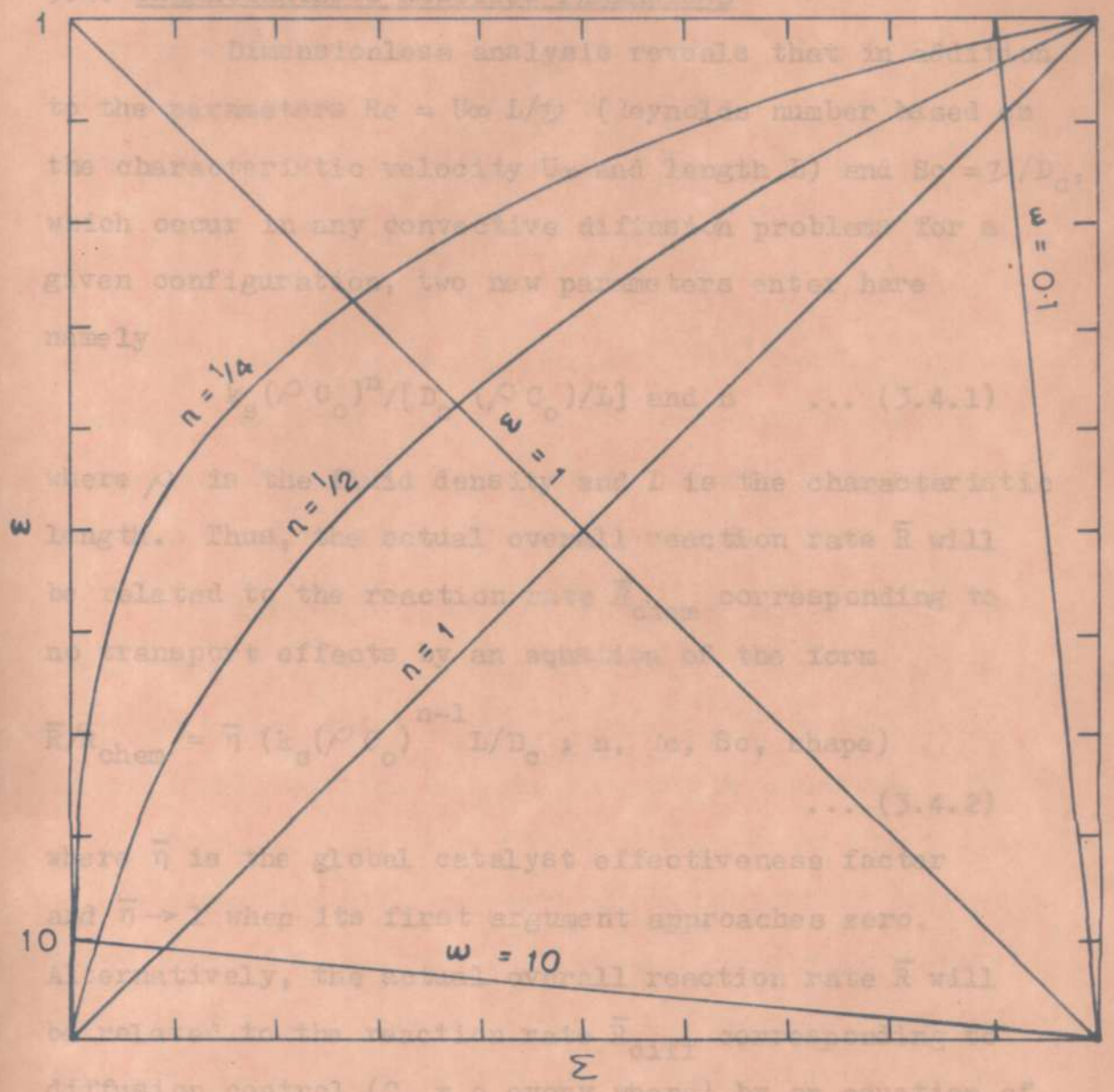


FIG. 3.4 / GRAPHICAL METHOD FOR THE SOLUTION OF CONVECTIVE DIFFUSION EQUATION WITH CHEMICAL REACTION

3.4. CHARACTERISTIC REACTION PARAMETERS

Dimensionless analysis reveals that in addition to the parameters $Re = U_{\infty} L/\nu$ (Reynolds number based on the characteristic velocity U and length l) and $Sc = \nu/D_c$, which occur in any convective diffusion problems for a given configuration, two new parameters enter here namely

$$k_s (\rho C_o)^n / [D_c (\rho C_o) / L] \text{ and } n \quad \dots (3.4.1)$$

where ρ is the fluid density and L is the characteristic length. Thus, the actual overall reaction rate \bar{R} will be related to the reaction rate \bar{R}_{chem} corresponding to no transport effects by an equation of the form

$$\bar{R} / \bar{R}_{chem} = \bar{\eta} (k_s (\rho C_o)^n / [D_c (\rho C_o) / L])^{n-1} \dots (3.4.2)$$

where $\bar{\eta}$ is the global catalyst effectiveness factor and $\bar{\eta} \rightarrow 1$ when its first argument approaches zero.

Alternatively, the actual overall reaction rate \bar{R} will be related to the reaction rate \bar{R}_{diff} corresponding to diffusion control ($C_o = 0$ everywhere) by an equation of the form

$$\bar{R} / \bar{R}_{diff} = \bar{\phi} (k_s (\rho C_o)^n / [D_c (\rho C_o) / L])^{n-1} ; n, Re, Sc, Shape \dots (3.4.3)$$

where $\bar{\phi}$ is the global correction for finite catalyst activity and $\bar{\phi} \rightarrow 1$ when its first argument approaches infinity.

Since the average Sherwood number \overline{Sh} for the same configuration is a function of Re and Sc alone, with no loss in generality, the first of the two new parameters, [equation (3.4.1)] may be replaced by

$$\overline{C}_n \equiv k_s (\rho C_o)^n \cdot L / [\overline{Sh} (Re, Sc.) D_c (\rho C_o)] \quad \dots (3.4.4)$$

where \overline{C}_n , the catalytic parameter for n^{th} order surface reaction has the evident interpretation of being the characteristic rate of interfacial reaction divided by the characteristic rate of convection diffusion.

For very small values of the basic dimensionless group \overline{C}_n , the reaction rate \overline{R} will be very close to its maximum value $\overline{R}_{\text{chem}}$, since, owing to the slow interfacial reaction and the favourable conditions of convection, the reactant concentration C_o at the fluid/solid interface will be everywhere negligibly different from the concentration C_o existing in the supply system. For intermediate values of \overline{C}_n , the steady state reactant concentration C , will drop below that existing in the supply system, and this is associated with a reduction of the overall reaction rate \overline{R} to a value less than $\overline{R}_{\text{chem}}$ (i.e. $\overline{\eta} < 1$). If one were unaware of this reactant depletion effect, the chemical surface reaction would appear to be characterized by a (smaller) rate constant

$$K = \bar{R} / [\rho C_0]^n S = \bar{\eta} \cdot k_s \quad \dots (3.4.5)$$

where S is the wetted area of the catalyst. However, in practice, even at constant surface temperature, the apparent rate constant K , would depend upon the conditions of convective diffusion (through $\bar{\eta}$). This has important implications for experiments designed to obtain the value of the true activation energy E , particularly at elevated surface temperatures. If the actual rate \bar{R} is different from \bar{R}_{chem} , then the apparent activation energy E_a so determined will be less than the true activation energy E , and, moreover, E_a will depend upon conditions of convective diffusion. This imply

$$E_a/E = 1 + (\partial \ln \bar{\eta} / \partial \ln \bar{C}_n) \quad \dots (3.4.6)$$

and owing to the properties of the $\bar{\eta}(\bar{C}_n, n)$ relation, it will be seen that E_a may be identified with E only in the limit $\bar{C}_n \rightarrow 0$, whereas $E_a \rightarrow 0$ as $\bar{C}_n \rightarrow \infty$. One can correct for the effect of convective diffusion in activation energy measurements only if the dependence of $\bar{\eta}$ on \bar{C}_n is known and if the value of $\bar{\eta}$ is determined.

The four characteristic reaction parameters defined and discussed above are summarised belows:

- (1) \bar{C}_n = The catalytic parameter
 The characteristic rate of interfacial
 = reaction.
 The characteristic rate of convective
 diffusion

$$= \frac{\bar{R}_{\text{chem}}}{\bar{R}_{\text{diff}}} = \frac{k_s}{k_g} = \frac{\text{true reaction rate constant}}{\text{mass transfer coefficient}}$$

(2) $\bar{\eta}$ = The integrated diffusion (effectiveness) factor

$$= (1 + \bar{C}_n) = (1 + \frac{k_s}{k_g})^{-1} = \frac{k_g}{k_s + k_g} = \frac{C_1}{C_0}$$

where C_1 = Surface concentration of the reactant

C_0 = Bulk concentration of the reactant

(3) $\bar{\phi}$ = Global cocorrection for finite catalyst activity

$$= \frac{\text{Actual overall rate}}{\text{Diffusion limited rate}}$$

$$= \bar{C}_n \cdot \bar{\eta} = \frac{k_s}{k_g} \cdot \frac{k_g}{k_s + k_g} = \frac{k_s}{k_s + k_g}$$

(4) $\frac{E_a}{E}$ = Normalized apparent activation energy

$$= 1 + (\partial \ln \bar{\eta} + \partial \ln \bar{C}_n)$$

$$= \bar{\eta} \quad \text{for } n = 1.$$

CHAPTER 4

DESCRIPTION OF THE APPARATUS

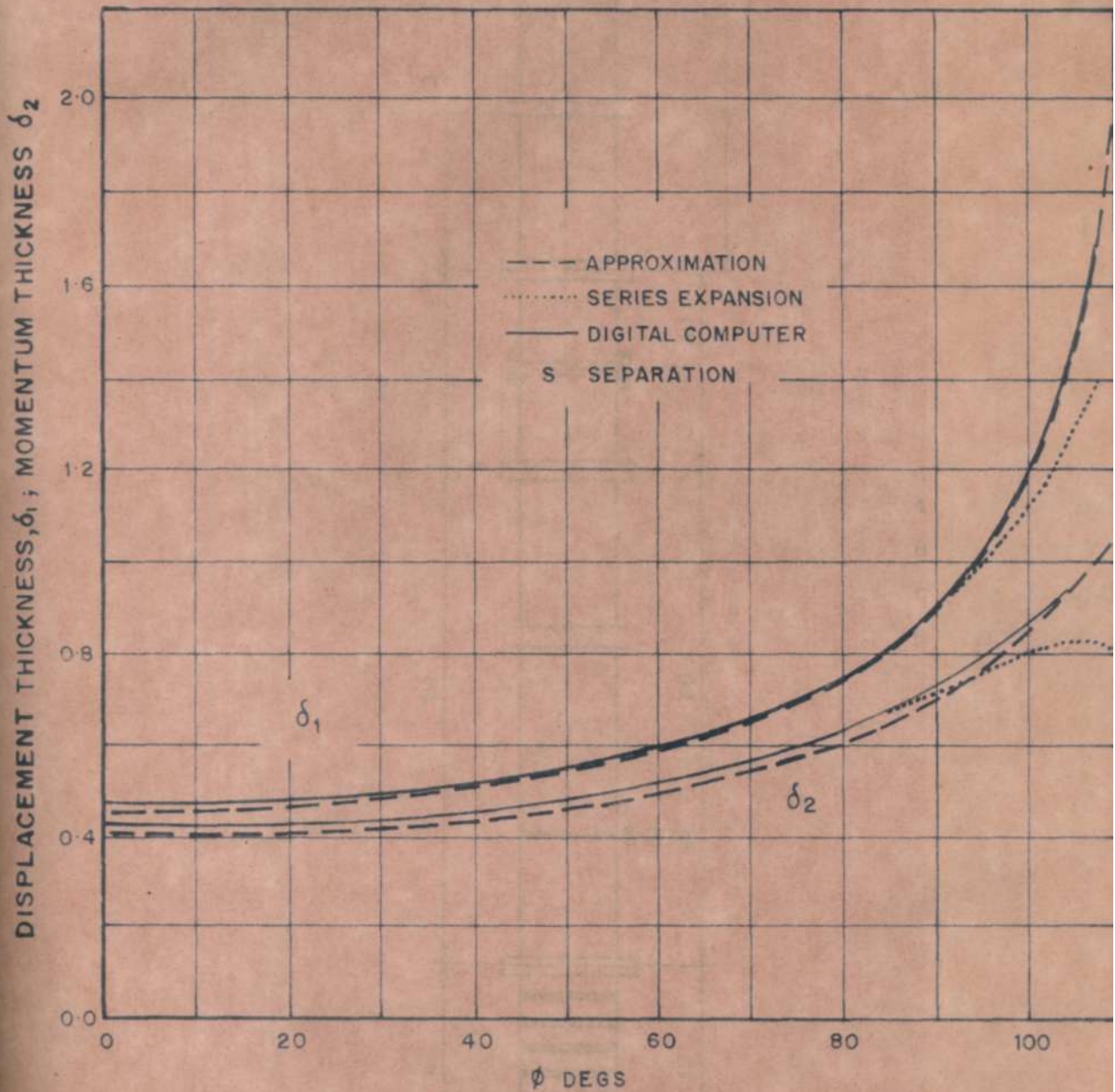
4.1. STAGNATION REGION OF A CIRCULAR CYLINDER - A WELL DEFINED FLOW FIELD

It is a formidable task to generate a uniform flow over a surface. The flow in a pipe has a parabolic velocity distribution, (Fig.4.3) as shown and the velocity is uniform at any position. If the coating is done over a radial distance of 20 per cent of the whole cylinder the variation in the velocities (between the mean velocity and the actual velocity) is of the order of 2 to 3 per cent. It is also seen from Fig.4.1, that by restricting the stagnation region to 30 degrees the variation in the displacement thickness and momentum thickness with position around the cylinder is negligible.

Thus, (i) by resorting to pipe flow and generating a parabolic velocity distribution, (ii) by coating the surface to a radial distance of 20 per cent of the whole cylinder and (iii) by restricting the stagnation region to 30 degrees the flow is well defined and the hydrodynamic solutions are helpful to study the flow in the stagnation region.

4.2. DESCRIPTION OF THE APPARATUS

The apparatus built for this investigation comprised a cylindrical G.I. duct (inside diameter 5.27 cm.) and had a total length of 1.8 m. A schematic diagram is shown in Fig.4.2. The calming section



δ_1 = DISPLACEMENT THICKNESS

δ_2 = MOMENTUM THICKNESS

FIG. 4-1 VARIATION OF DISPLACEMENT THICKNESS, δ_1 , AND MOMENTUM THICKNESS, δ_2 WITH POSITION AROUND THE CIRCULAR CYLINDER

consisted of two screens made up of two 40 mesh
 followed by three 100 mesh screens. The purpose of the
 screens was to interrupt the flow and destroy the
 boundary layer at the wall. The entrance section
 was 1 m. length ($L = 20D$) and the downstream 0.8 m.

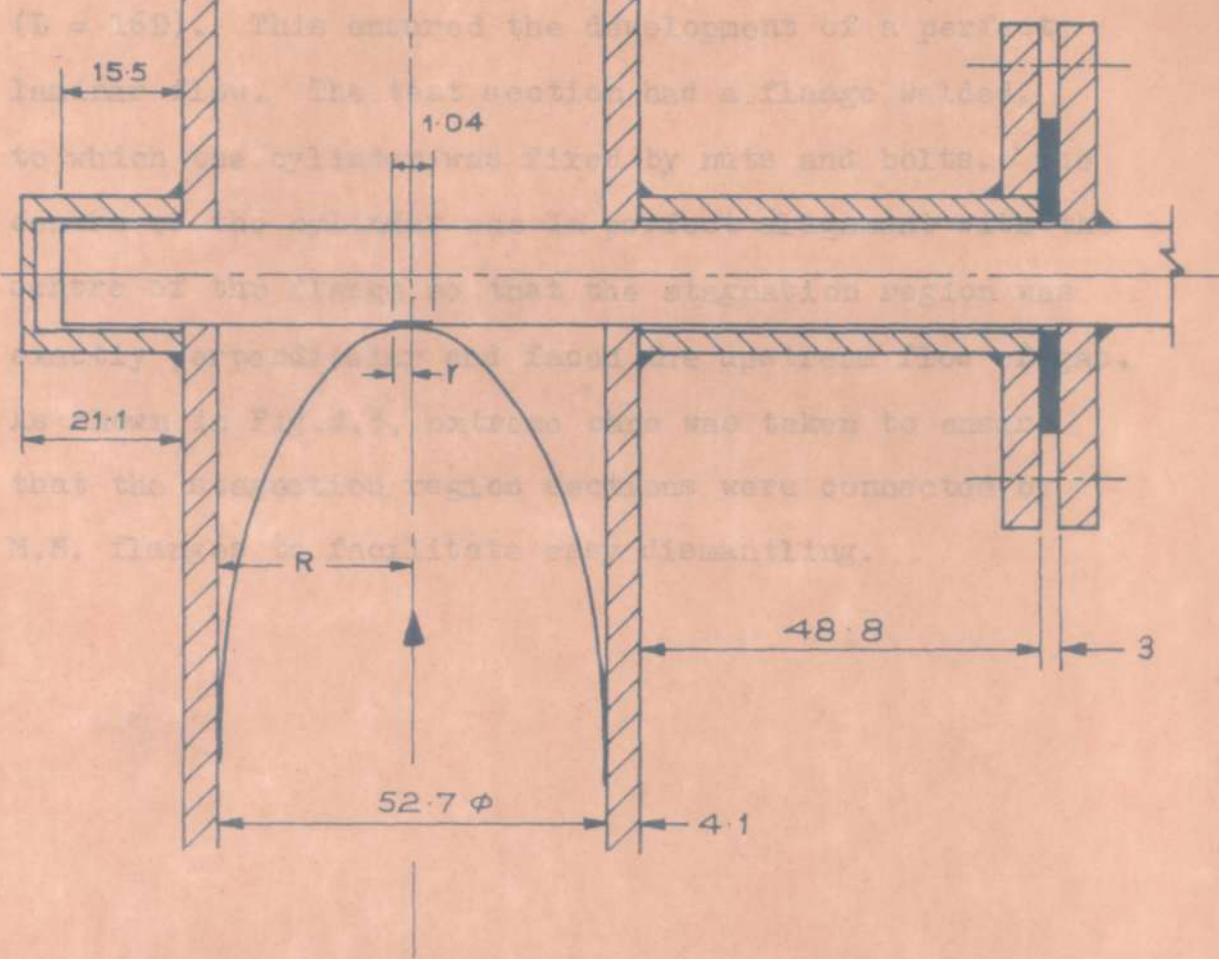


FIG. 4-3 TEST SECTION (ENLARGED VIEW)

ALL DIMENTIONS ARE IN MILLIMETRES)

consisted of five screens made up of two 40 mesh followed by three 100 mesh screens. The purpose of the screens was to smoothen out the flow and destroy the boundary layer at the duct walls. The entrance section was 1 m. in length ($L = 20D$) and the downstream 0.8 m. ($L = 16D$). This ensured the development of a perfect laminar flow. The test section had a flange welded, to which the cylinder was fixed by nuts and bolts. The centre of the cylinder was in perfect alignment with the centre of the flange so that the stagnation region was exactly perpendicular and faced the upstream flow of gas. As shown in Fig.4.3, extreme care was taken to ensure that the stagnation region sections were connected by M.S. flanges to facilitate easy dismantling.

CHAPTER 5

MASS TRANSFER EXPERIMENTS

Mass transfer studies were carried out over naphthalene coated surface. The rate of mass transfer was measured and compared with the mass transfer rate determined theoretically. This was to check the validity of the theoretical calculations.

5.1. PURIFICATION OF NAPHTHALENE

Chemically pure naphthalene was dissolved in rectified spirit (95 per cent ethanol) and recrystallized. The recrystallized sample was then sublimed and very pure naphthalene free from other impurities was obtained. It had a melting point of 80.5° C.

5.2. COATING OF NAPHTHALENE IN THE STAGNATION REGION

The purified naphthalene was filled up to 3/4th of a big test tube and slowly heated in a waterbath, and when a clear solution was obtained, the clean stainless steel cylinder was slowly dipped for a minute and taken out. A thin uniform coating of naphthalene was obtained on the cylinder. It was then slowly cut with a sharp knife and the coating in other parts of the cylinder was removed, leaving a little more than the required area in the stagnation region. The excess area was then carefully covered with a cellophane tape. The cellophane tape not only helped in getting the exact area required for exposure but also supported the coating in the stagnation region.

5.3. METHOD OF ANALYSIS

The concentration of naphthalene obtained by the experiments was of the order of 10^{-5} gm.moles/litre. To measure this quantity accurately, the outcoming naphthalene in air was absorbed in rectified spirit (spectrophotometric grade) and the concentration of naphthalene was determined by measuring the absorbance in a UV Spectrophotometer (Fig. 5.1). Since naphthalene has an extinction coefficient of 10^4 at $\lambda = 286$, the concentration was accurately determined from the calibration chart (Fig,5.2).

5.4. EXPERIMENTAL SET UP AND PROCEDURE

The experimental set up for mass transfer studies is shown in Fig.5.3. Air from the cylinder (dried over anhydrous magnesium perchlorate) was fed to the reactor through calibrated capillary flow meters. The flow rate was adjusted for the required Reynolds number. After about an hour, when the system was in a steady state, the outlet E of the duct was connected to series of absorbers (provided with spargers at the inlet as shown in the Figure) filled with spectroscopic grade rectified spirit. Air was blown for a known interval of time and the rectified spirit was made up to known volume and the concentration of naphthalene was determined. Before the commencement of every run, air was blown in the duct for

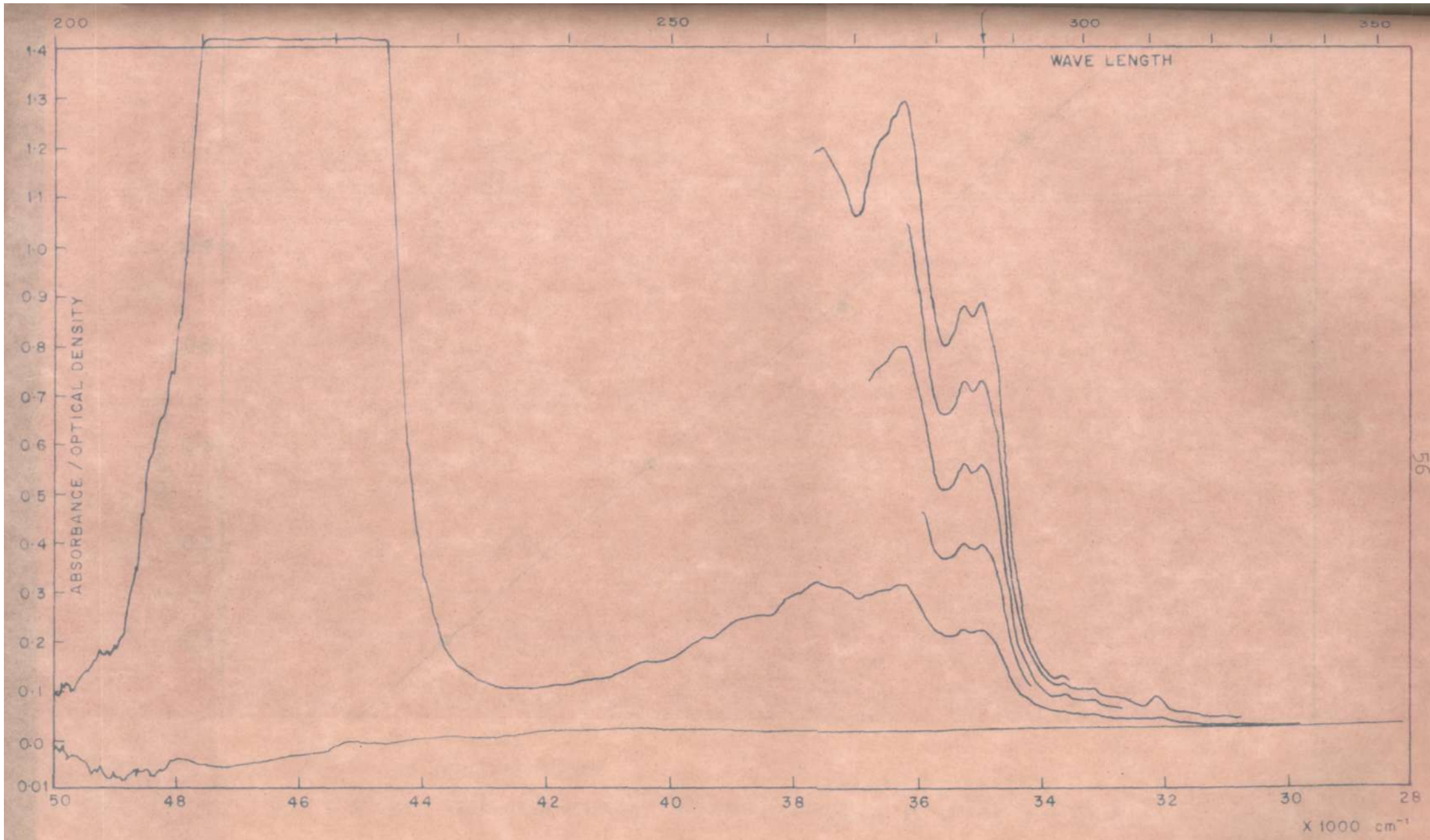


FIG. 5-1 SPECTRUM OF NAPHTHALENE IN RECTIFIED SPIRIT AT VARIOUS CONCENTRATIONS AT $\lambda = 286$

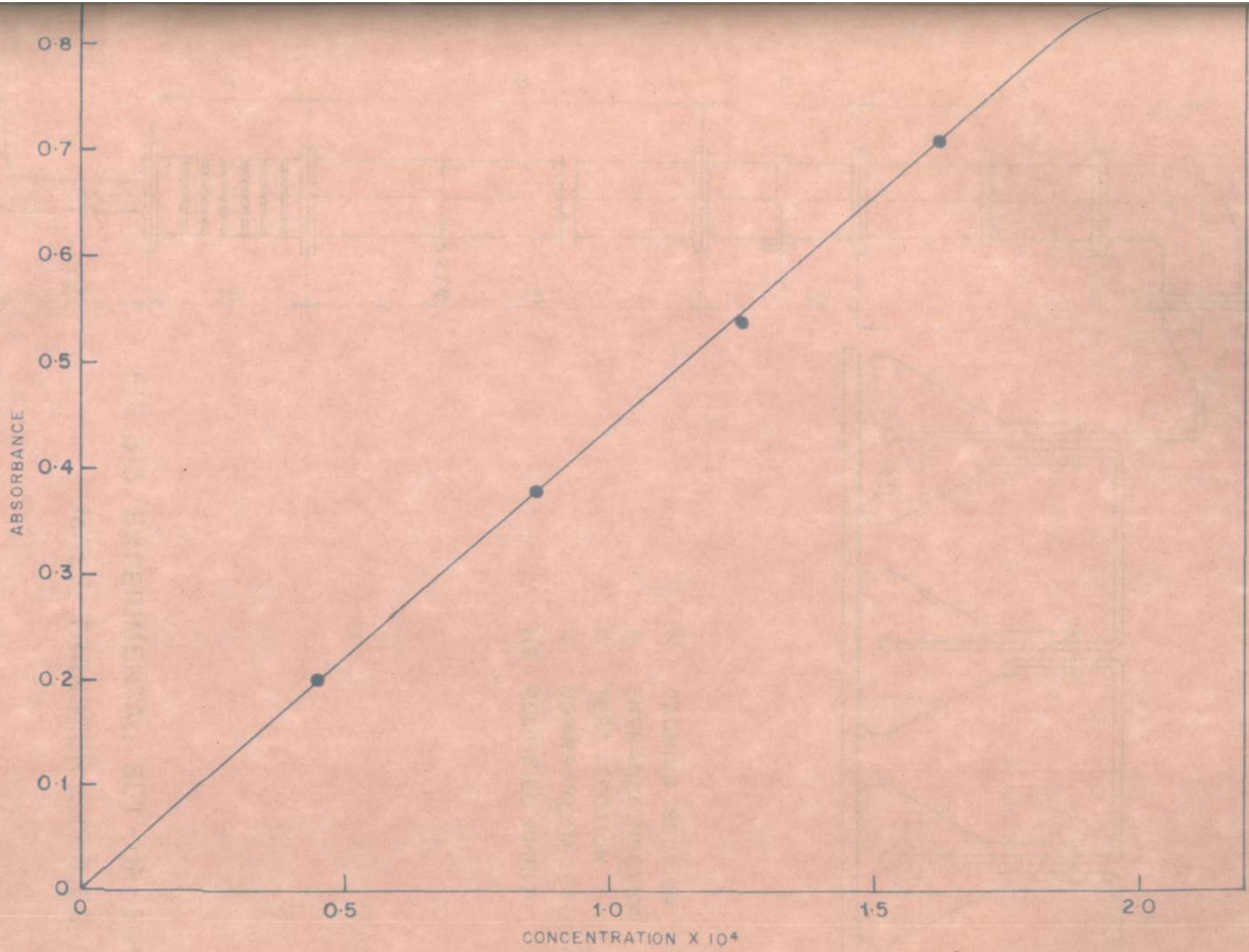


FIG. 5.2. CALIBRATION CHART - CONCENTRATION OF NAPHTHALENE
Vs ABSORBANCE .

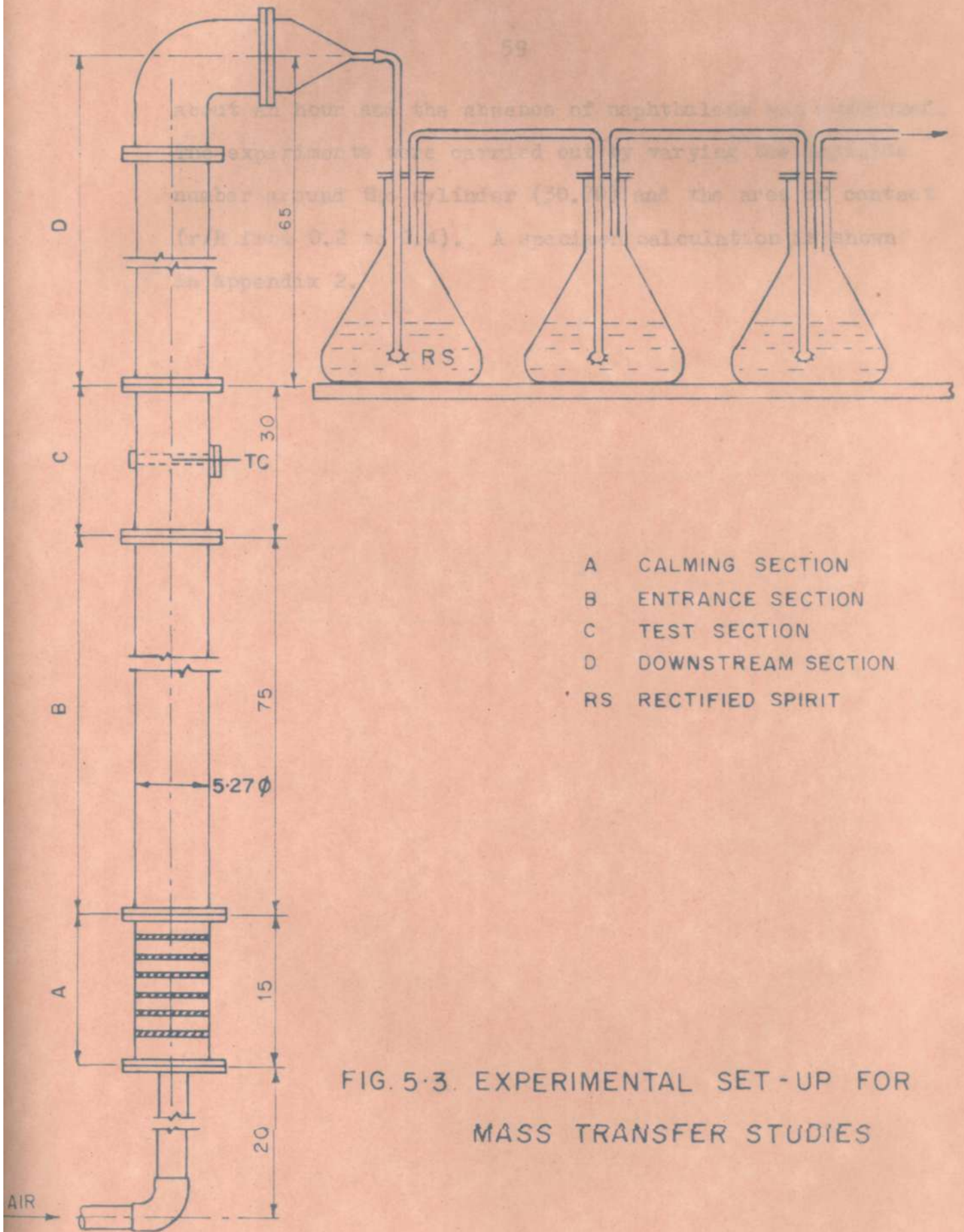


FIG. 5.3. EXPERIMENTAL SET-UP FOR MASS TRANSFER STUDIES

about an hour and the absence of naphthalene was confirmed. The experiments were carried out by varying the Reynolds number around the cylinder (30.70) and the area of contact (r/R from 0.2 to 0.4). A specimen calculation is shown in Appendix 2.

CHAPTER 6

KINETIC EXPERIMENTS

The reaction between hydrogen and oxygen (air) was chosen as the chemical process primarily for the following reasons:

(1) Our object is to operate the reaction in the intermediate regime where both chemical kinetics and diffusion govern the observed reaction rate. The reaction between hydrogen and oxygen is known to be very fast and affected by both diffusion and reaction.

(2) There is a large difference between the thermal conductivity of hydrogen and air. The concentration of hydrogen in the circulating reactants can be easily determined by a thermal conductivity detector.

(3) Platinum, which is widely used as the catalyst for this reaction is very active and its deposition techniques on a metallic surfaces are well known,

(4) The reactants, hydrogen and air are readily available, easy to handle and stored in cylinders.

(5) The reaction has been studied extensively and the kinetics are available in literature.

6.1. DEPOSITION OF PLATINUM IN THE STAGNATION REGION

Platinum was deposited by evaporated metal film technique as described below:

About 0.5 gms. of platinum wire was taken and cut into small pieces. These pieces were kept on

a tungsten filament which had provision for electrical heating. The stainless steel cylinder was first cleaned by trichloroethylene followed by methanol and acetone in the ultrasonic cleaner. The cylinder was covered with aluminium foil and only the required area was exposed. It was then put on a ring holder and supported on a stand, which was about 10 cms. above the tungsten filament. The glass dome was put over the unit and a vacuum of 10^{-6} Torr was applied inside. The platinum metal was then deposited by heating the tungsten filament for about 2 to 3 minutes. This procedure was repeated 10 to 15 times. Degassing was done intermittently and some time was allowed for obtaining the required vacuum. The vacuum was released slowly and the cylinder was taken out. The required area was found to be uniformly coated and the coating had a bright finish.

6.2. CATALYST ACTIVITY

The question of catalyst activity is of prime consideration and the surface activity was maintained by pretreating the platinum surface at 150° C before every run in dry air for one hour.

6.3. METHOD OF ANALYSIS

The composition of hydrogen in air was determined by the specially built thermal conductivity detector by taking advantage of the large difference

between the thermal conductivity of air and hydrogen. The sample was introduced into the gas analyzer with the help of a hypodermic gas tight syringe. Known samples of hydrogen in air were introduced into the TCD and the corresponding deflection measured in the strip chart recorder. From this calibration chart (Fig.6.1) the unknown composition of hydrogen in air in the circulation gas mixture was determined.

6.4. EXPERIMENTAL SET UP AND PROCEDURE

The experimental set up for kinetic studies is shown in Fig.6.2. Air and hydrogen from the cylinder (dried over anhydrous magnesium perchlorate) were fed to the reactor through separate metering systems and mixed at the entrance to the reactor. The reactants were circulated by a diaphragm pump in conjunction with a surge tank. The gases were trapped in the circulation line by suitable adjustments of the valves shown in the diagram. The flow in the circulation line was adjusted by means of a needle valve provided in the suction side of the pump and the flow rate was accurately measured by means of a rotameter. The initial concentration of hydrogen in the circulation was adjusted to be around 3 per cent. Temperature control of the reactor and air and hydrogen mixture was obtained with three separate heating sections and the temperature of the reactor was

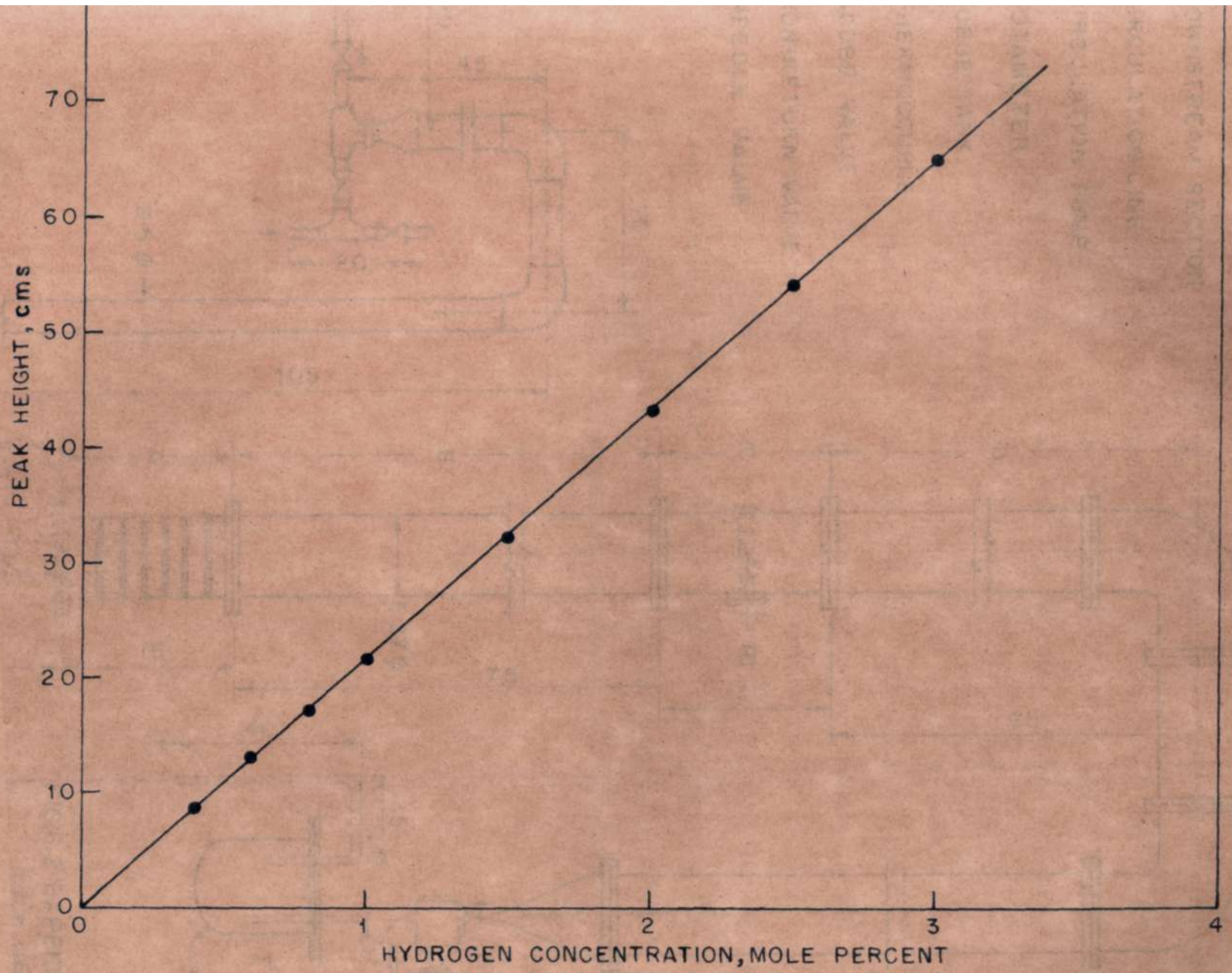
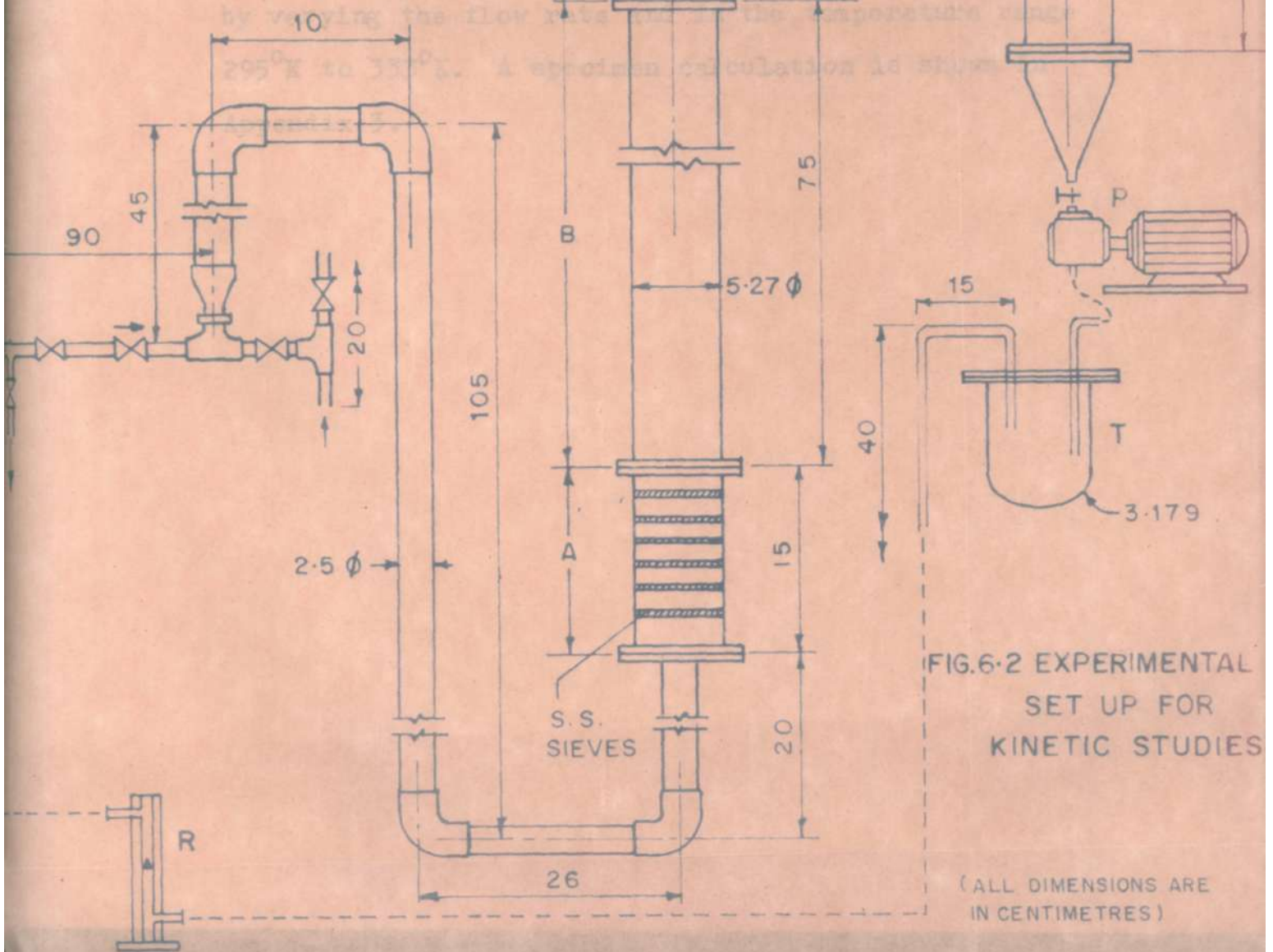


FIG. 6-1 CALIBRATION CHART - HYDROGEN CONCENTRATION Vs PEAK HEIGHT

- A CALMING SECTION
 B ENTRANCE SECTION
 C TEST SECTION
 D DOWNSTREAM SECTION
 E CIRCULATION LINE
 P CIRCULATION PUMP
 R ROTAMETER
 T SURGE TANK
 TC THERMOCOUPLE
 ⊗ GLOBE VALVE
 ⊗ NON-RETURN VALVE
 T NEEDLE VALVE



measured by a copper-constantan thermocouple inserted on the cylinder and located exactly above the stagnation region. When the flow and temperature became steady, samples were withdrawn from the circulation line at known intervals by a hypodermic gas tight syringe. In every case 1.5 ml. sample was used with air as the carrier gas. Mole per cent of hydrogen present in the sample was indicated¹ by the deflection (peak height) measured in the strip chart recorder. The experiments were carried out for Reynolds number (Re_D) between 40-70, by varying the flow rate and in the temperature range 295°K to 333°K. A specimen calculation is shown in Appendix 3.

CHAPTER 7

RESULTS AND DISCUSSION

MASS TRANSFER EXPERIMENTS

Mass transfer experiments were carried out over the naphthalene coated surface by varying the Reynolds number around the cylinder and the area of contact. The rate of mass transfer was measured and compared with the mass transfer determined theoretically. The results are tabulated in Table 2. The Sherwood number for mass transfer calculated theoretically (equation 3.1.29) and measured experimentally are plotted against the Reynolds number around the cylinder. The plots are shown in Figures 7.1, 7.2 and 7.3. The deviation between the theory and experiments were well within 5 per cent, thus confirming the validity of the theoretical expressions.

KINETIC EXPERIMENTS

The reaction between hydrogen and oxygen catalysed by platinum was studied over the temperature range 295° - 333° K and feed concentration of hydrogen in the range 0 to 3 per cent in air. Due to the continuous circulation of the reactants, the reaction was subjected to batch reactor analysis and the concentration of hydrogen in the circulating reactants was measured at known intervals and the plot is shown in Fig.7.4. A plot of $-\ln(1-X_A)$ vs time (minutes) was made as shown

TABLE 2

Expt. No.	Temp. o _K	Time hrs.	C _s x 10 ⁻⁸ gm. moles /cm ³	D _c cm ² /sec.	A _c
1.	296.4	2.0	0.3965	0.06450	0.6541
2.	297.7	2.0	0.4480	0.06504	0.6541
3.	296.9	2.5	0.4156	0.06471	0.6541
4.	296.8	1.5	0.4117	0.06463	0.6541
5.	297.0	2.0	0.4195	0.06475	0.6541
6.	298.4	2.0	0.4781	0.0653	1.3082
7.	298.6	2.0	0.4870	0.0654	1.3082
8.	299.0	1.5	0.5054	0.06559	1.3082
9.	298.1	1.5	0.4649	0.0652	1.3082
10.	297.1	1.5	0.4235	0.06479	1.3082
11.	298.7	2.0	0.4916	0.06546	0.98115
12.	298.0	2.0	0.4606	0.06517	0.98115
13.	299.0	2.0	0.5054	0.06559	0.98115
14.	298.9	1.5	0.5008	0.06555	0.98115
15.	299.2	1.5	0.5148	0.06567	0.98115

TABLE 2 (Contd.)

Expt. No.	sh _D (theory)	sh _D (expt.)	Re _D	Deviation per cent
1.	11.2049	11.1560	6.9282	-0.4364
2.	10.022	10.247	6.1967	+2.2450
3.	8.6793	8.4875	5.3665	-2.2090
4.	12.2744	11.9701	7.5894	-2.4791
5.	13.2579	13.4347	8.1975	+1.3335
6.	10.4813	10.4144	6.4807	-0.6382
7.	11.4816	11.3509	7.0992	-1.1383
8.	9.3747	9.7416	5.7965	+3.9137
9.	8.1187	8.0247	5.0199	-1.1578
10.	12.4016	12.5752	7.6681	+1.3998
11.	10.9092	10.7223	6.7453	-1.7132
12.	11.9505	11.7896	7.3891	-1.4300
13.	12.9080	12.2771	7.9812	-4.8876
14.	9.7575	9.8820	6.0332	+1.2759
15.	8.4502	8.7222	5.2249	+3.2188

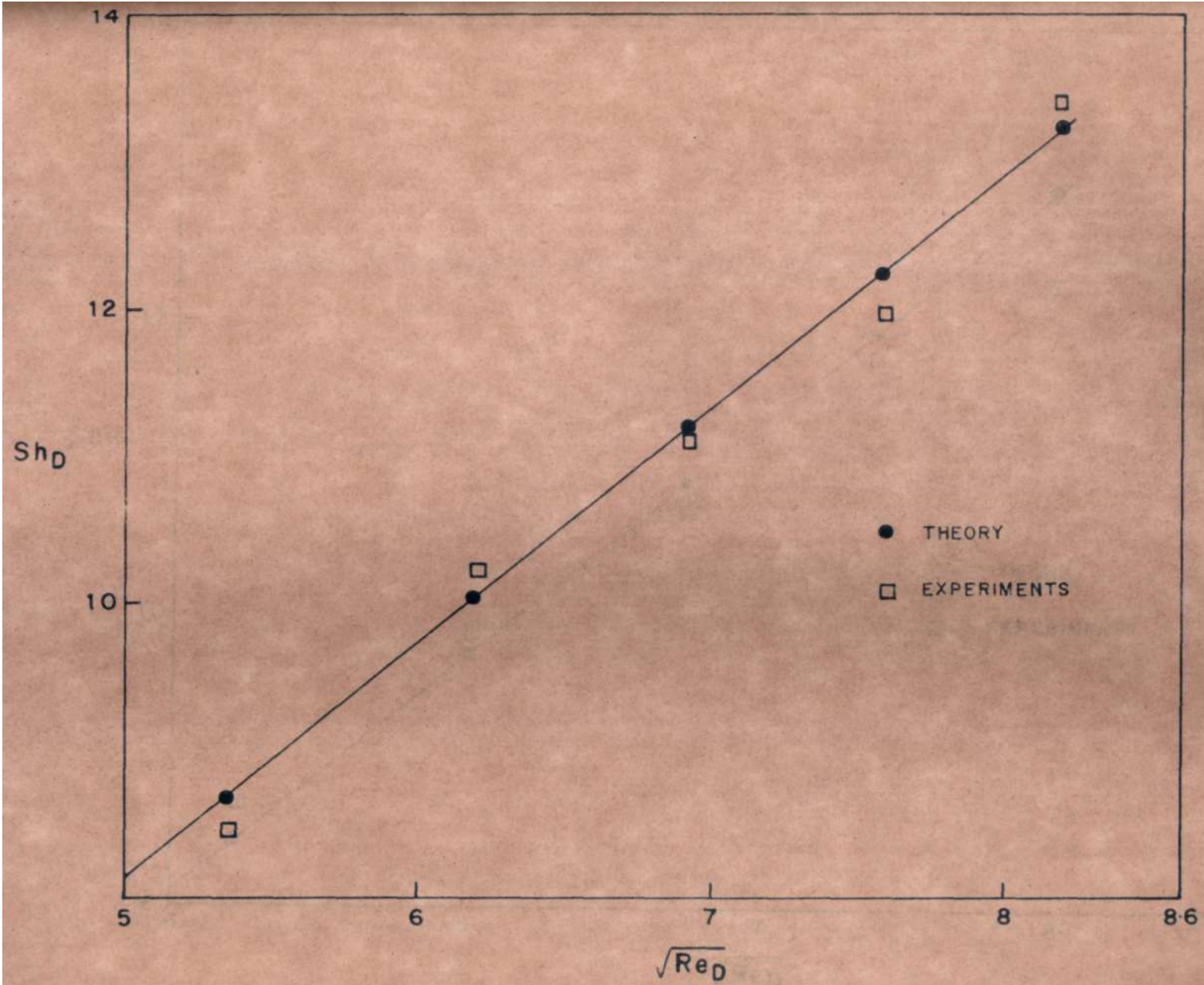


FIG. 7-1. MASS TRANSFER AROUND THE STAGNATION REGION
THEORY AND EXPERIMENTS, $r = 0.2 R$.

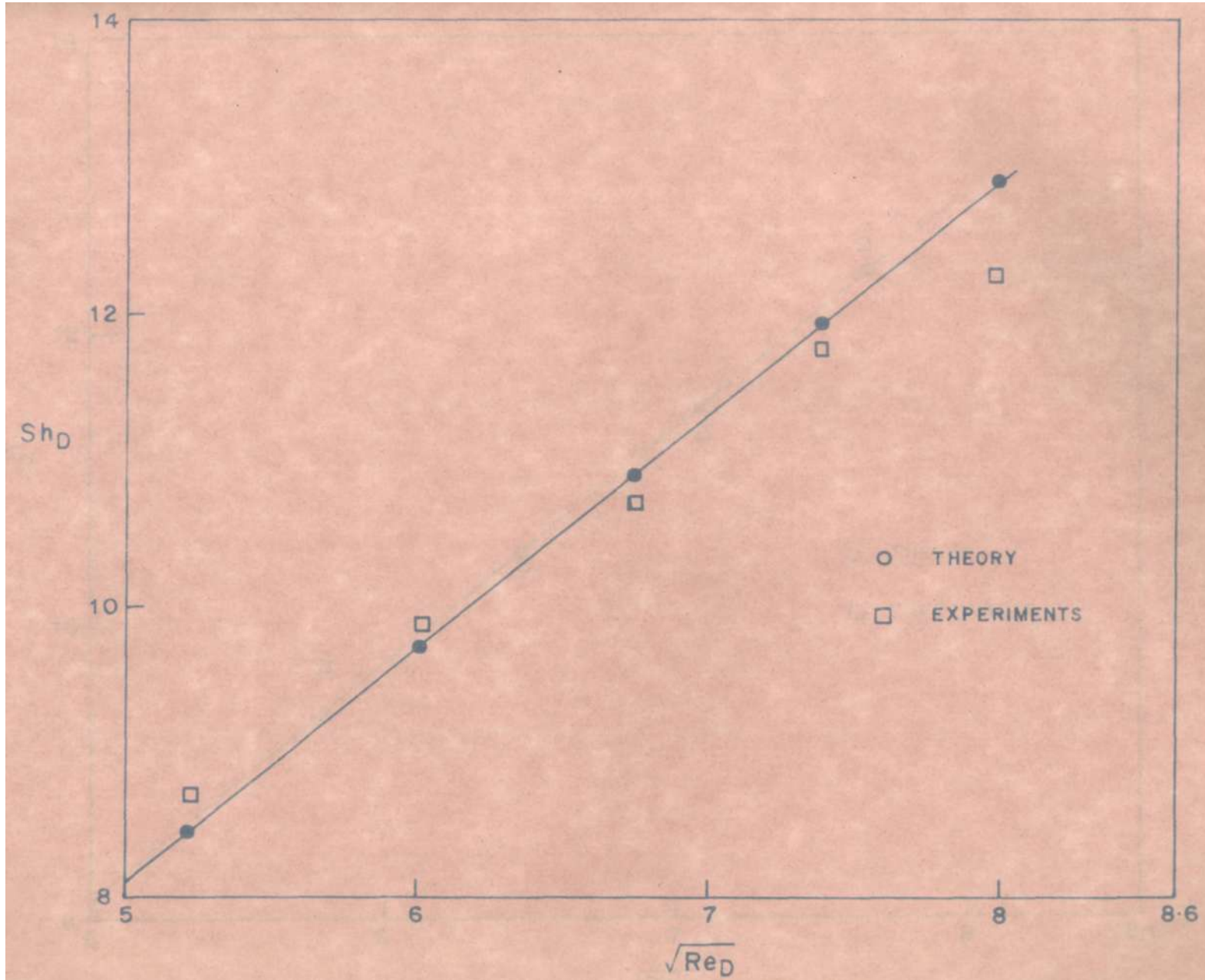


FIG. 7.2. MASS TRANSFER AROUND THE STAGNATION REGION, THEORY AND EXPERIMENTS. $r = 0.3 R$.

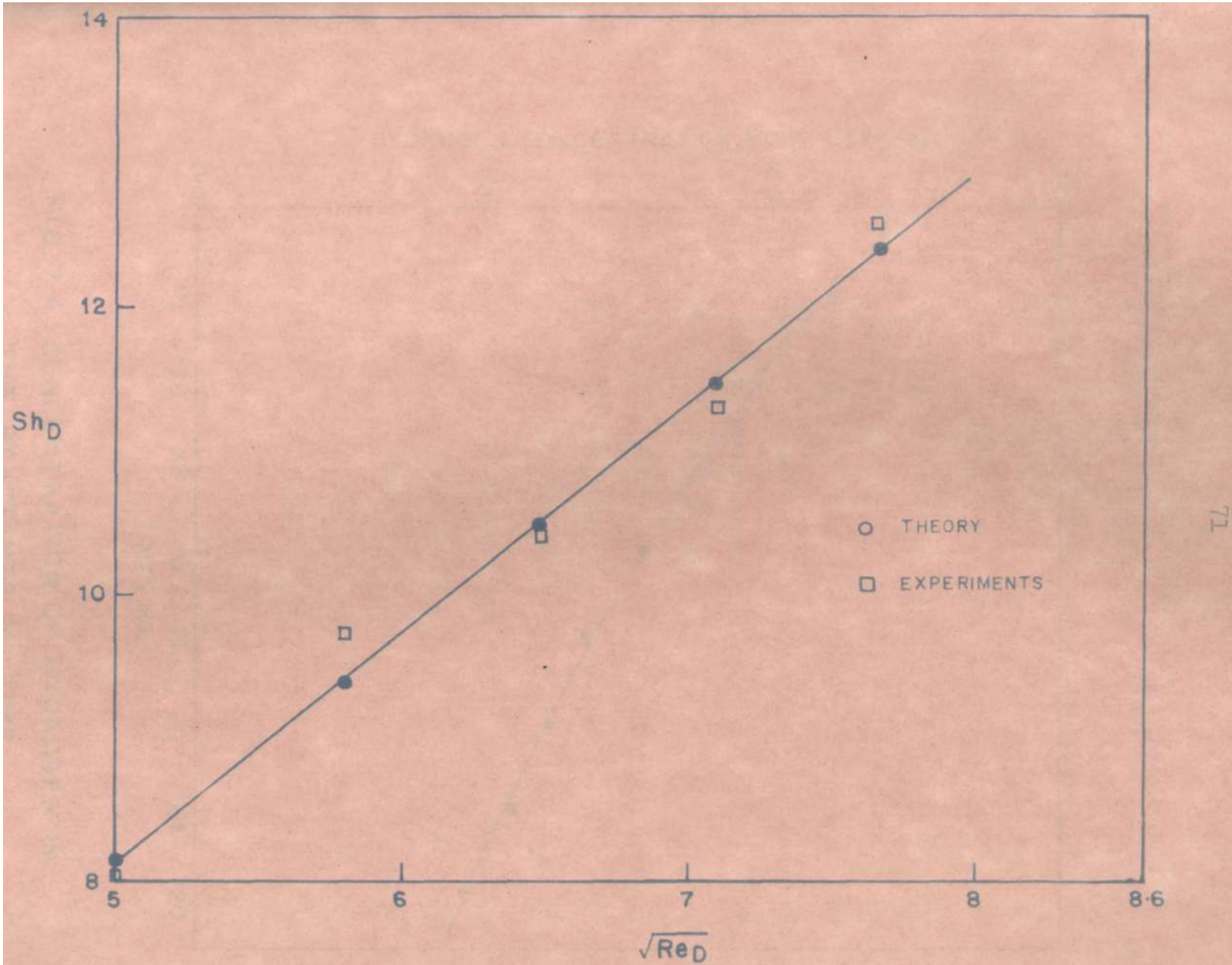


FIG. 7.3. MASS TRANSFER AROUND THE STAGNATION REGION,
THEORY AND EXPERIMENTS. $r = 0.4 R$.

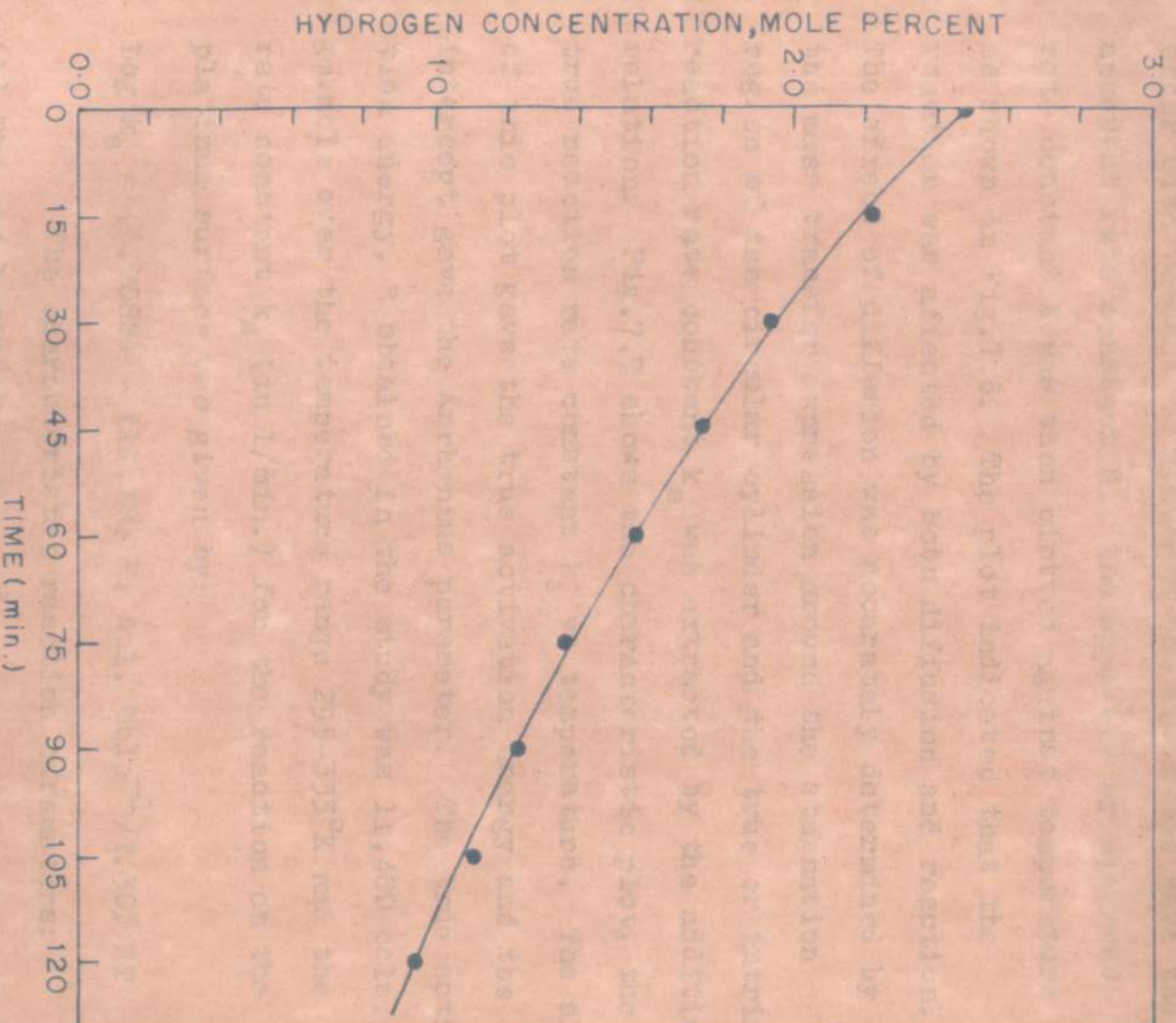


FIG. 7.4 CONCENTRATION OF HYDROGEN IN
THE REACTANTS VS TIME

in Fig.7.5. It gave a straight line passing through the origin. This indicated that the reaction was first order with respect to hydrogen and its slope gave the apparent rate constant K . The apparent or observed rate constant K was then plotted against temperature as shown in Fig.7.6. The plot indicated that the reaction was affected by both diffusion and reaction. The effect of diffusion was accurately determined by the mass transfer expression around the stagnation region of the circular cylinder and the true or intrinsic reaction rate constant k_s was extracted by the additivity relation. Fig.7.7 shows the characteristic plot, the true reaction rate constant k_s vs temperature. The slope of this plot gave the true activation energy and the intercept gave the Arrhenius parameter. The true activation energy, E obtained in the study was 11,480 cal./gm.mole over the temperature range 295-333° K and the rate constant k_s (in l/min.) for the reaction on the platinum surface was given by:

$$\text{Log } k_s = (6.2088) - (11.48) K. \text{ col. mole}^{-1}/2.303 RT$$

The characteristic reaction parameters:

- (1) The catalytic parameter, C_n
- (2) The integrated diffusion (effectiveness) factor η
- (3) The Global correction for finite-catalyst activity θ and
- (4) The normalized apparent activation energy, E_a/E

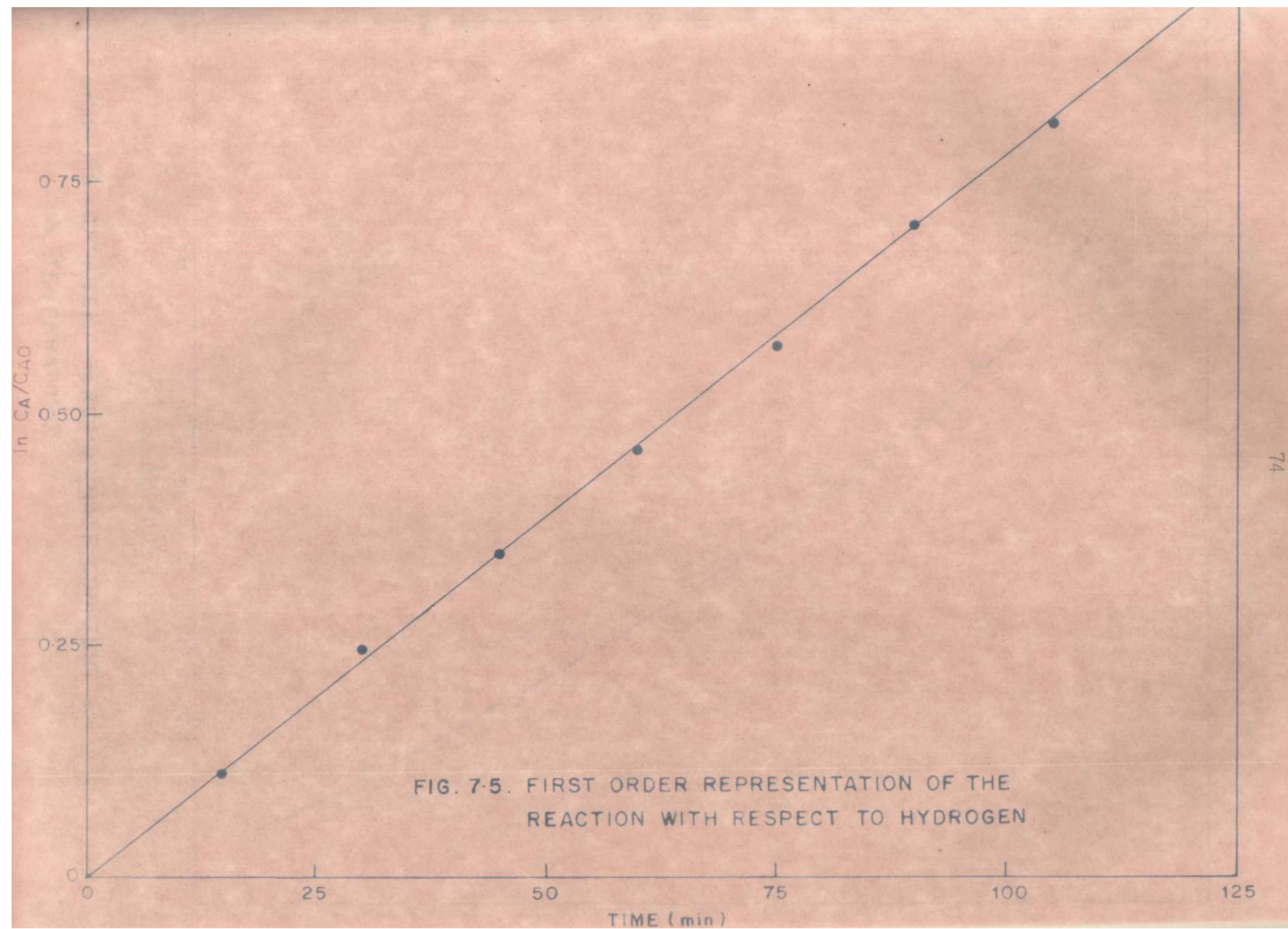


FIG. 7-5. FIRST ORDER REPRESENTATION OF THE REACTION WITH RESPECT TO HYDROGEN

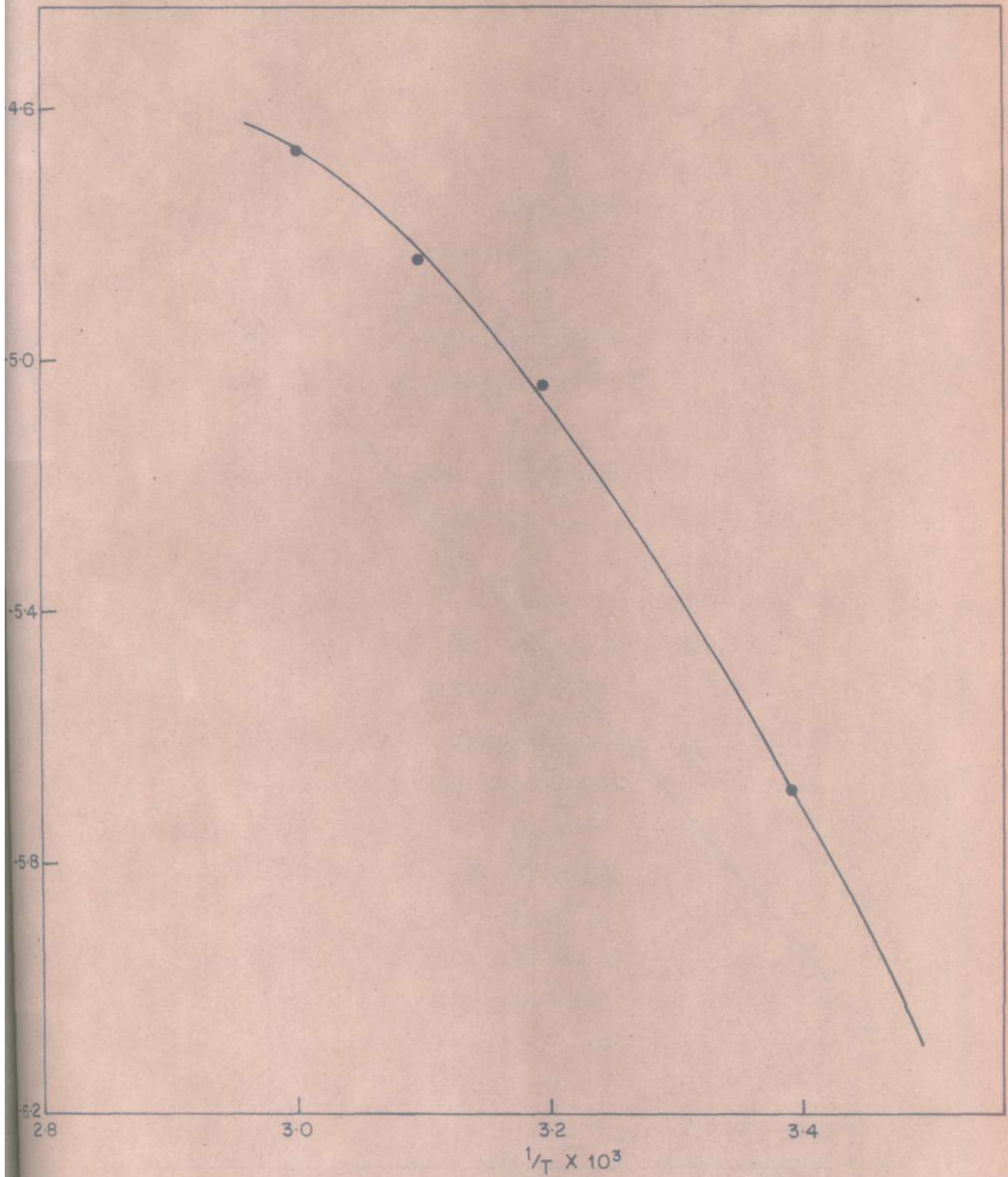


FIG. 7.6. APPARENT REACTION RATE CONSTANT K
Vs TEMPERATURE.

defined and discussed in Chapter 6 were evaluated and the results were tabulated (Table 4).

The following characteristics plots were prepared:

(1) \ln (catalytic parameter $\bar{\eta}_2$) vs \ln (integrated diffusion factor $\bar{\eta}$) ... Fig. 7.8

(2) Integrated diffusion (effectiveness) factor $\bar{\eta}$ vs normalized apparent activation energy, E_a/R ... Fig. 7.9

(3) The global conversion for finite catalyst activity \bar{Y} vs (integrated diffusion (effectiveness) factor $\bar{\eta}$) ... Fig. 7.10

The above results of the kinetic experiments may be discussed in relation to the reported experiments in the literature on the same system.

Boroskov (1954) studied the reaction between hydrogen and oxygen and reported an activation energy of 10 ± 2 K cal./gmole on platinum. Under conditions of continuous drying and low conversion Boroskov found the reaction to proceed according to first order kinetics. Boroskov used a differential bed recycle reactor in which only differential conversion took place at one end part through the catalyst. Gidaspov and Illington (1964) in their work on reaction of hydrogen with excess air on platinum catalyst reported first order

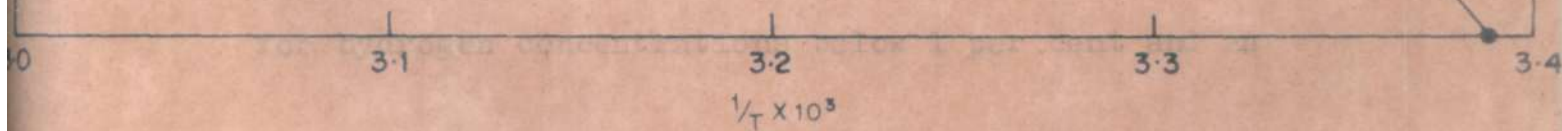


FIG 7.7. TRUE REACTION RATE CONSTANT k , Vs TEMPERATURE

defined and discussed in Chapter 3 were evaluated and the results were tabulated (Table 3).

The following characteristics plots were prepared:

- (1) \ln (catalytic parameter \bar{c}_n) vs \ln (Integrated diffusion factor $\bar{\eta}$) ... Fig.7.8
- (2) Integrated diffusion (effectiveness) factor $\bar{\eta}$ vs normalized apparent activation energy, E_a / E ... Fig.7.9
- (3) The Global correction for finite catalyst activity $\bar{\phi}$ vs Integrated diffusion (effectiveness) factor $\bar{\eta}$... Fig.7.10

The above results of the kinetic experiments may be discussed in relation to the reported experiments in the literature on the same system.

Boroskov (1954) studied the reaction between hydrogen and oxygen and reported an activation energy of $10 + 2 K$ cal./gm.mole on platinum. Under conditions of continuous drying and low conversion Boroskov found the reaction to proceed according to first order kinetics. Boroskov used a differential bed recycle reactor in which only differential conversion took place at any one part through the catalyst. Gidasov and Ellington (1964) in their work on reaction of hydrogen with excess air on platinum catalyst reported first order for hydrogen concentrations below 1 per cent and an

TABLE 3

Run No.	Room temp. K	Total flow rate (air + hydrogen) at room temp, LMP	Reaction temp. $^{\circ}\text{K}$ hr.sq.cm.	Observed or apparent rate constant K (gm.mole/ atm.)	Mass transfer coefficient k (gm.mole/ hr.sa.cm. atm.)
1.	295	4.03	295	0.1425	0.4262
2.	297	4.12	313	0.2588	0.4354
3.	298	4.12	323	0.3067	0.4410
4.	296	4.09	333	0.3586	0.4460
5.	294	3.25	294	0.1339	0.3810
6.	297	3.29	313	0.2367	0.3901
7.	299	5.30	313	0.27259	0.4934

TABLE 3 (Contd.)

Run No.	True rate constant k_s (gm.mole/ hr.sq.cm. atm.)	$C\eta = k_s / k_g$	$\eta = k_g / k_s + k_g$	$\emptyset = k_s / k_s + k_g$	E_a	E_a / E
1.	0.2142	0.5025	0.6655	0.3344	7.630	0.6466
2.	0.6383	1.466	0.4055	0.5944	4.857	0.4230
3.	1.0069	2.2832	0.3045	0.6952	3.468	0.3021
4.	1.8298	4.1026	0.1959	0.8036	2.255	0.1964
5.	0.2066	0.5422	0.6484	0.3115	---	---
6.	0.6014	1.5416	0.3934	0.6064	---	---
7.	0.6091	1.2344	0.4475	0.5524	---	---

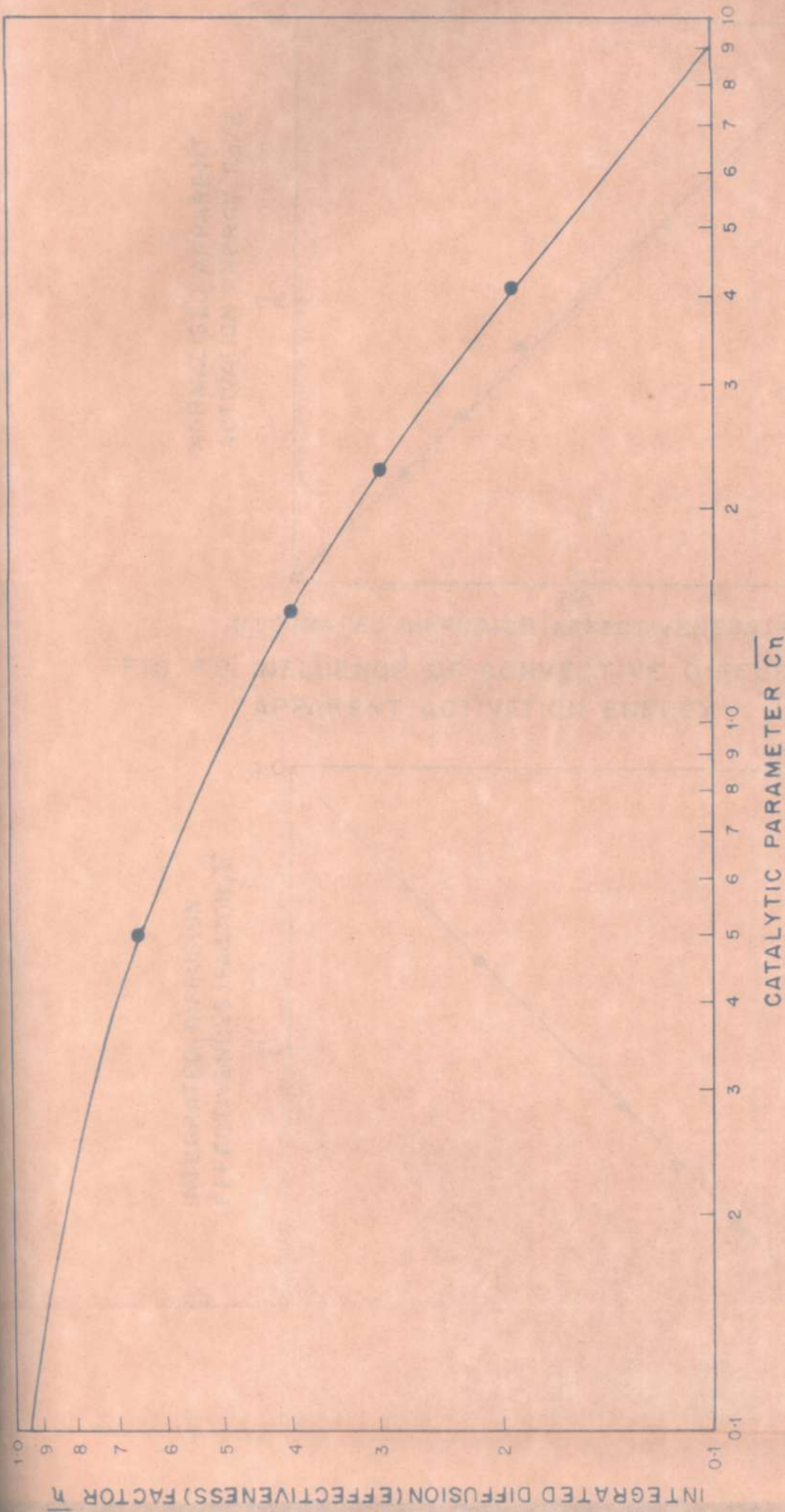


FIG. 7.8. DEPENDENCE OF INTEGRATED DIFFUSION (EFFECTIVENESS) FACTOR $\bar{\eta}$ ON CATALYTIC PARAMETER $\bar{C}\eta$

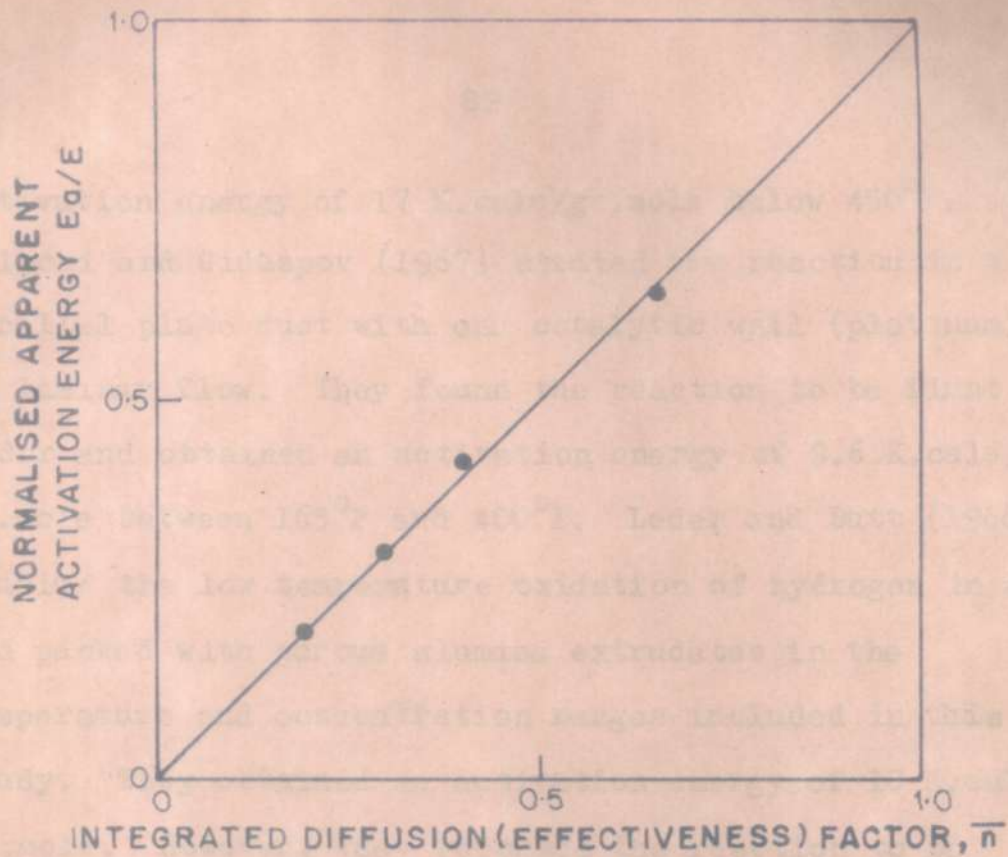


FIG. 7.9. INFLUENCE OF CONVECTIVE DIFFUSION ON APPARENT ACTIVATION ENERGY

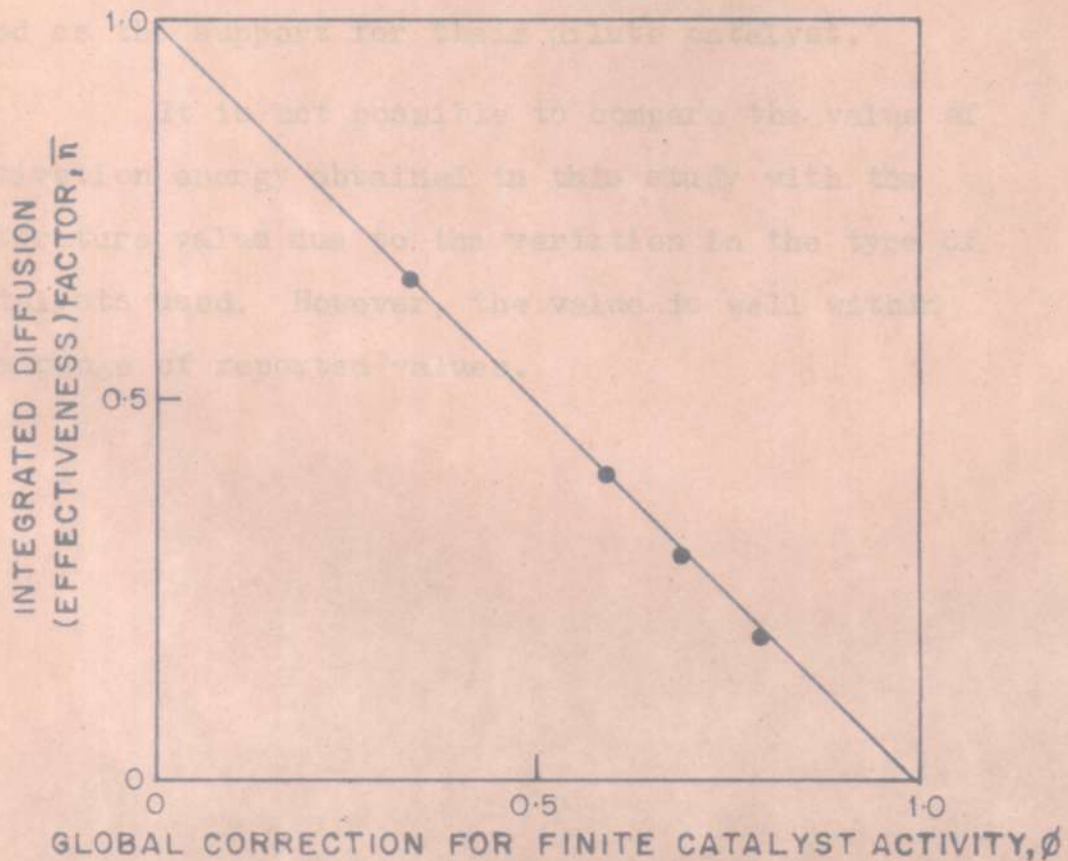


FIG. 7.10. GLOBAL CORRECTION FOR FINITE CATALYST ACTIVITY, ϕ Vs. INTEGRATED DIFFUSION (EFFECTIVENESS) FACTOR \bar{n}

activation energy of 17 K.cals/gm.mole below 450° F. Kulacki and Gidasov (1967) studied the reaction in a parallel plate duct with one catalytic wall (platinum) in laminar flow. They found the reaction to be first order and obtained an activation energy of 9.6 K.cals/gm.mole between 165°F and 400° F. Leder and Butt (1966) studied the low temperature oxidation of hydrogen in a bed packed with porous alumina extrudates in the temperature and concentration ranges included in this study. They obtained an activation energy of 10 K.cals/gm.mole. However, they reported the reaction to be second order. Their rate law may have differed due to water chemisorption in the surrounding alumina surface used as the support for their dilute catalyst.

It is not possible to compare the value of activation *energy* obtained in this study with the literature value due to the variation in the type of catalysts used. However, the value is well within the range of reported values.

CHAPTER 8

CONCLUSIONS

Our investigation would appear to be the first attempt to use the uniform accessibility quality in the stagnation region of a circular cylinder in an experimental study of transport limited heterogeneous catalysis and the following specific contributions have been made.

(1) Approximate analytical solutions for high and low Schmidt numbers for mass transfer to the stagnation region have been derived. They agree favourably with the exact solutions reported.

(2) Convective diffusion with a catalytic reaction in the stagnation region has been solved and a general expression for an n^{th} order reaction obtained.

(3) Mass transfer experiments have been conducted in a carefully designed stagnation flow set up. Naphthalene vaporization was used as the experimental system. The experimental data agreed well with the theoretical calculations.

(4) The reaction between hydrogen and oxygen catalyzed by platinum was studied over the temperature range 295 -333° K and at feed concentrations of hydrogen in the range 0 to 3 per cent in air. The reaction was found to be affected by both diffusion and reaction. The effect of diffusion was accurately determined by the

theoretical expression and the kinetic parameter extracted by the additivity relation. The reaction was found to be first order with respect to hydrogen and the true activation energy obtained in this study was 11,480 cal./gm.mole over the temperature range 295-333° K and the rate constant k_s (in 1/min.) for the reaction on the platinum surface was given by;

$$\log k_s = (6.2088) - (11.48) K \text{ cal. mole}^{-1} / 2.303 RT$$

(5) The characteristic reaction parameters were discussed, defined, calculated and the characteristic plots prepared.

This study indicates that the stagnation flow region of a cylinder can be a convenient system for studying the true kinetics of a solid catalyzed reaction due to its unique property of uniform accessibility.

APPENDIX 1

DIFFUSION COEFFICIENT OF HYDROGEN
IN AIR AND CALCULATION OF
SCHMIDT NUMBER

The diffusion coefficient of hydrogen in air (D_c) is reported to be

$$D_c = 3.7788 \times 10^{-5} \times T^{1.75} \text{ at 1 atmosphere}$$

[Marrco and Mason (1972)]

At barometric pressure of 708.8 mm Hg.

$$D_c = 3.7788 \times 10^{-5} \times \frac{760}{708.8} \times T^{1.75}$$

$$= 4.0517 \times 10^{-5} \times T^{1.75}$$

The kinematic viscosity of air (ν) is reported to be;

$$\nu = 7.256 \times 10^{-6} \times T^{1.75} \text{ at 1 atmosphere}$$

[Hilsenrath et al. (1960)].

At barometric pressure of 708.8 mm Hg.

$$\nu = 7.256 \times \frac{760}{708.8} \times 10^{-6} \times T^{1.75}$$

$$= 7.780 \times 10^{-6} \times T^{1.75}.$$

$$\text{Schmidt number } Sc = \frac{\nu}{D_c} = \frac{7.780 \times 10^{-6} \times T^{1.75}}{4.0517 \times 10^{-5} \times T^{1.75}} = 0.198$$

$$= 0.2$$

[Reported value 0.22°, Refs Spalding (1963)]

APPENDIX 2
MASS TRANSFER EXPERIMENTS
SPECIMEN CALCULATION

(i) Calibration of Specord UV Spectrophotometer - Naphthalene in rectified spirit

Concentration gm. mole/litre x 10 ⁻⁴	Absorbance/optical density (at $\lambda = 286$)
0.45	0.20
0.86	0.38
1.24	0.54
1.62	0.71
2.00	0.87

According to Beer's Law $A = \epsilon Cd$.

where A = Absorbance or optical density

ϵ = Extinction coefficient or specific extinction

C = Concentration of naphthalene in gm.moles / litre .

d = Cell path in cms.(= 1 cm. for Specord),

A plot of absorbance vs concentration is made as shown in Fig.5.2. The slope gives the extinction coefficient.

Slope from plot = $\epsilon = 4342$; $\log \epsilon = 3.637$

[Reported value: $\log \epsilon$ at $\lambda = 286$, for naphthalene in rectified spirit = 3.65)].

[Ref : Silverstein and Bassler (1963)].

(ii) Diffusion coefficient of, naphthalene, in air D_c) and its variation with temperature T .

The diffusion coefficient can be estimated by the correlation:

$$D_c = \frac{0.001858 \times T^{3/2} [M_1 + M_2] / M_1 M_2^{1/2}}{P \sigma_{12}^2 \Omega_D} \dots (1)$$

where T is the absolute temperature ($^{\circ}\text{K}$), M_1 , M_2 are the molecular weights of the two species, P is the total pressure (atm.), V_b is the 'collision integral', a function of kT/ϵ_{12} , $\epsilon\sigma$ are the force constants in the Lennard-Jones potential function, and k is the Boltzmann constant. [Ref: Satterfield (1970)].

$$\left(\frac{M_1 + M_2}{M_1 M_2}\right)^{1/2} = \left(\frac{128.16 + 28.96}{128.16 \times 28.96}\right)^{1/2} = 0.205.$$

$$\sigma_{12} = \frac{1}{2} (\sigma_1 + \sigma_2) \quad \dots (2)$$

Since σ_1 , for naphthalene is not known, it is calculated by the following correlation (Ref: Satterfield, page 16).

$$\sigma_1 = 1.18 V_b^{1/3} \quad \dots (3)$$

where V_b is the liquid molal volume at the normal boiling point ml. V_b is estimated by Nenson's method [Ref: Reid and Sherwood, 1966)].

$$\frac{V_c}{V_b} = 0.422 \log_{10} P_c + 1.981 \quad \dots (4)$$

where V_c = Critical molal volume, ml/gm. mole

P_c = Critical pressure, atm.

For naphthalene :

$V_c = 3.1847$ ml/gm. $P_c = 29792$ mm Hg and

$t_c = 469^{\circ}\text{C}$.

[Ref: Physical Properties of Chemical Compounds', 1955 ACS., Washington, p. 203)].

$$V_c = 3.1847 \times 128.16 = 408.15 \text{ ml./gm.mole.}$$

$$P_c = 29792/760 = 39.2 \text{ atmospheres.}$$

Substituting these values in equation (4)

$$\frac{408.15}{V_b} = 0.422 \log (39.2) + 1.981$$

$$= 0.6724 + 1.981 = 2.6534.$$

$$V_b = 408.15/2.6534 = 153.82 \text{ ml./gm.mole.}$$

$$\sigma_1 = 1.18 (153.82)^{1/3} = 1.18 \times 5.358 = 6.322 \text{ \AA}^{\circ}$$

$$\sigma_2 = 1.18 \text{ (for air)} = 3.711 \text{ \AA}^{\circ} \text{ (Satterfield, p.14)}$$

$$\sigma_{12} = \frac{1}{2} (6.322 + 3.711) = 5.0165 \text{ \AA}^{\circ}.$$

$$\sigma_{12}^2 = 25.165.$$

The value of Ω_D collision integral is a function of kT/ϵ_{12}

where k = Boltzmann constant.

ϵ_{12} = Force constant in the Lennard - Jones potential function

$$\epsilon_{12} = \sqrt{\epsilon_1 \epsilon_2} \quad \dots \quad (6)$$

[Satterfield, p.17].

For naphthalene value of ϵ_1 is not available and is estimated by the empirical equation

$$kT/\epsilon_1 = 1.30 \frac{T}{T_c} \quad \dots \quad (6)$$

[Satterfield p.16]

i.e. $k/\epsilon_1 = 1.3/T_c \quad \dots \quad (7)$

$$k/\epsilon_1 = 1.3/(273 + 469)$$

$$\epsilon_1/k = 742/1.3 = 570.8^{\circ}\text{K}$$

For air $\epsilon_2/k = 78.6^\circ\text{K}$ (Satterfield, p.14)

$$\begin{aligned} k/\epsilon_2 &= \sqrt{\frac{k}{\epsilon_1} \frac{k}{\epsilon_2}} \\ &= \sqrt{\frac{1}{570.8} \frac{1}{78.6}} = \frac{1}{211.8} \end{aligned}$$

At 300°K , $\frac{kT}{e_{12}} = \frac{300}{211.8} = 1.4164$

The values of collision integral Ω_D in the range 1.35 to 1.45 are tabulated along with the corresponding temperature for the system [Ref : Satterfield, p.14]

$\frac{kT}{\sigma_{12}}$	Ω_D	T°K	°C
1.35	1.253	285.9	12.9
1.40	1.233	296.5	23.5
1.45	1.215	307.1	34.1

(iii) Variation of diffusion coefficient (of naphthalene in air) with temperature

From equation (1)

$$\frac{(D_c)_{T_1}}{(D_c)_{T_2}} = \left(\frac{T_1}{T_2}\right)^{3/2} \left(\frac{(\Omega_D)_{T_2}}{(\Omega_D)_{T_1}}\right) \quad \dots(8)$$

Since Ω_D is a function of temperature only for a given system, the above equation can be reduced as

$$\frac{(D_c)_{T_1}}{(D_c)_{T_2}} = \left(\frac{T_1}{T_2}\right)^a \quad \dots(9)$$

The value of exponent 'a' is worked out as follows:

$$\frac{(\Omega_D)_{T_2}}{(\Omega_D)_{T_1}} = \left(\frac{T_1}{T_2}\right)^b \quad \dots \quad (10)$$

Substituting the values of Ω_D and T in equation (10)

$$\frac{1.253}{1.233} = \left(\frac{296.5}{285.9}\right)^b$$

i.e. $1.0162 = 1.0371^b$

$$b = \log (1.0162 / \log 1.0371) = 0.4412$$

Similarly $\frac{1.233}{1.216} = \left(\frac{307.1}{296.5}\right)^b$

$$b = 0.4185$$

The variation in exponent b is small and hence from the desired temperature range of 23.4 to 34°C

(i.e. $\frac{kT}{\epsilon_{12}} = 1.4$ to 1.45)

Value of b is taken as 0.42.

Value of a = $1.5 + 0.42 = 1.92$

$$\frac{(D_c)_{T_1}}{(D_c)_{T_2}} = \left(\frac{T_1}{T_2}\right)^{1.92} \quad \dots (11)$$

The value of D_c at 296.5°K is calculated by substituting the value of Σ_{12} , Ω_D in equation (1)

$$D_c \text{ at } 296.5^\circ\text{K} = 0.0603 \text{ cm}^2/\text{sec.}$$

$$D_c \text{ at } 298^\circ\text{K} = 0.0603 \left(\frac{298}{296.5} \right)^{1.92}$$

$$= 0.061084 \text{ cm}^2 / \text{sec.}$$

[reported value = 0.0611 Ref: C.N.Satterfield , p.13]

$$D_c \text{ at } 300^\circ\text{K} = 0.0603 \left(\frac{300}{296.5} \right)^{1.92} = 0.0616 \text{ cm}^2/\text{sec.}$$

Kinematic viscosity ν at any temperature T

$$= 7.256 \times 10^{-6} \times T^{1.75}$$

$$\nu \text{ at } 300^\circ\text{K} = 0.15688 \text{ cm}^2/\text{sec.}$$

$$\text{Schmidt number, } Sc = \nu/D_c = \frac{0.15688}{0.0616} = 2.546$$

[Reported value 2.55 Ref. Spalding (1963)]

(iv) Vapour pressure of naphthalene

The vapour pressure of naphthalene can be estimated by the correlation

$$\log p_v = \frac{-3722.5}{T} + 11.424 \quad (16 \text{ to } 51^\circ\text{C})$$

(Gildenblut et al. 1960)

$$P_v = \frac{2.655 \times 10^{11}}{10^{3722.5/T}}$$

Concentration of naphthalene $C_s = P_v / R_T$ at the surface

$$= \frac{2.655 \times 10^{11}}{10^{3722.5/T} \times 6.236 \times 10^4 \times T} \text{ gm. mole/cm}^3$$

(v) Estimation of Sherwood number Sh_D (Run. No.1)

Average temperature during the course of the experiment (2 hrs.) = $23.4^\circ\text{C} = 296.4^\circ\text{K}$.

Flow rate at $23.4^\circ\text{C} = 4$ lit. per minute.

Reynolds number in the pipe $Re_p = \frac{DU_\infty}{\nu}$

where D is the diameter of the pipe

U , is the linear velocity of air in the pipe

$$\frac{4000}{60 \times \frac{\pi}{4} \times (5.27)^2} \text{ cm./sec.}$$

ν = kinematic viscosity of air

$$= 7.780 \times 10^{-6} \times 296.4^{1.75}$$

$$Re_p = \frac{DU_\infty}{\nu} = \frac{5.27 \times 4,000}{60 \times \frac{\pi}{4} \times (5.27)^2 \times 7.780 \times 10^{-6} \times 296.4^{1.75}}$$

$$= 97.96$$

The average velocity around the coated surface

$$(r/R = 0.2) U_{av.} = \frac{Q}{\pi (0.2R)^2} = \int_0^{0.2R} 2U \left[\frac{1-(r/R)^2}{\pi (0.2R)^2} \right] 2\pi r \cdot dr$$

$$U_{av} = 1.96 U$$

Reynolds number around the cylinder Re_D

$$= \frac{1.96}{4} Re_p = 0.49 Re_p$$

$$= 0.49 \times 97.96 = 48.00$$

$$\sqrt{Re_D} = \sqrt{48} = 6.9282$$

Concentration of naphthalene at the surface C_s

$$\begin{aligned}
 &= \frac{2.655 \times 10^{11}}{10^{3722.5/296.4}} \\
 &= \frac{2.655 \times 10^{11}}{6.236 \times 10^4 \times 296.4} \\
 &= 0.3965 \times 10^{-8} \text{ gm. moles/cm}^3
 \end{aligned}$$

Diffusivity coefficient of naphthalene at 296.4° K and 710 mm. Hg.

$$\begin{aligned}
 D_c &= 0.0603 \times \left(\frac{296.4}{296.5}\right)^{1.92} \times \frac{760}{710} \\
 &= 0.06450 \text{ cm}^2 / \text{sec.}
 \end{aligned}$$

Area of the coated surface, $A_c = \frac{1}{6} \times \pi \times 1.25 \times 1$
 $= 0.6541 \text{ sq.cm.}$

Absorbance / optical density from UV Spectrophotometer = 0.19.

Rate of mass transfer from the calibration chart.,

Pig. 5.2 = 0.43×10^{-4} gm. moles/litre.

Since the rectified spirit was made upto 250 ml, the actual rate of mass transfer of naphthalene j

$$= \frac{0.43 \times 10^{-4}}{4} = 0.1075 \times 10^{-4} \text{ gm. moles}$$

$$j = k_g C_s A_c \times t = Sh_D \times \frac{D}{D_c} \times C_s \times A_c \times t$$

where k_g is the mass transfer coefficient in cm/sec.

C_g is the concentration of naphthalene at the surface gm.moles/cm³

A_c is the area of the coated surface in cm².

Sh_D is the Sherwood number for mass transfer around the cylinder.

D_c is the diffusion coefficient of naphthalene in cm^2/sec .

D is the diameter of the cylinder

t is the time of collection in secs.

$$\begin{aligned} sh_D(\text{experimental}) &= \frac{j}{C_s \cdot A_c \cdot t} \times \frac{D}{D_c} \\ &= \frac{0.1075 \times 10^{-4}}{0.39.65 \times 10^{-8} \times 0.6541 \times 2 \times 3600} \times \frac{1.25}{0.0645} \\ &= 11.1560 \end{aligned}$$

In the stagnation region of a circular cylinder we have shown

$$\frac{1}{2} \frac{Sh_D}{\sqrt{Re_D}} = F(Sc) \quad \dots \text{Equation 3.1.29)}$$

For $Sc = 2.5$, $F(Sc) = 0.80865$ (from Table 1, Chapter 3).

$$\begin{aligned} Sh_D(\text{theoretical}) &= 2 \times \sqrt{Re_D} \times F(Sc) \\ &= 2 \times 6.9282 \times 0.80865 \\ &= 11.20498 \end{aligned}$$

Percentage deviation from the expression developed

$$= \frac{0.0489}{11.2049} \times 100 = 0.4364 \text{ per cent}$$

APPENDIX 3

TOTAL VOLUME OF THE REACTOR

TOTAL VOLUME OF THE REACTOR

	<u>Vol. ccs.</u>
1. 1.25 cms. dia. total length 250 cms.	306
2. 2.5 cms. dia. : total length 151 cms.	961
3. 5.27 cms. dia. : total length 300 cms.	6540
4. Tank - 15 cms. dia., 13 cms. length	3179
5. Conical portion	94
6. Rubber tube ; 120 cms. length 1 cm. dia.	120
	= = = =
	11200
	= = = =

Total volume of the reactor :11.2 litres.

APPENDIX 4
KINETIC EXPERIMENTS
SPECIMEN CALCULATION

KINETIC EXPERIMENTS

Specimen calculation (Run No.3)

- (1) Estimation of observed or apparent rate constant K,
 Room Temperature = 298° K, Flow rate of air and
 hydrogen at room temperature = 4.12 litres per minute,
 Reaction Temperature = 323° K.

Time.Mts. (t)	Peak Ht. (cms.)	Conc. of hydrogen mole per cent	-In (1 - XA) -In (CA/CA ₀)
0	53.5	2.48	0.0
15	48.0	2.22	0.1107
30	42.0	1.94	0.2455
45	37.5	1.75	0.3406
60	33.5	1.56	0.4635
75	29.0	1.36	0.5717
90	26.5	1.23	0.7012
105	23.5	1.10	0.8129
120	20.0	0.94	0.9701

A plot of - In CA/CA₀ VS. t (minutes) was made. It gave a straight line passing through the origin. This indicated that the reaction was first order with respect to hydrogen and its slope gave the observed or apparent rate constant K.

$$K = 0.0079127/\text{min.} = 0.4747/\text{hr.}$$

$$K \text{ in } \frac{\text{gm. mole}}{\text{hr. sq. cm. atm.}} = K \left(\frac{1}{\text{hr}} \right) \times \frac{V}{A_c \times R \times T}$$

where V is the total volume of the reactor = 11.2 litres
(Appendix 3).

A_c is the surface area of the coated catalyst.

R is the gas constant in litre atm./gm. mole °K

T is the reaction temperature in °K.

$$K = \frac{0.4747 \times 11.2}{0.6541 \times 0.08206 \times 323} = 0.3067 \frac{\text{gm. moles}}{\text{hr. sq. cm. atms.}}$$

(2) Estimation of true reaction rate constant k_s

Flow rate of air + hydrogen at 298°K = 4.12 LPM

Flow rate at 323°K = $4.12 \left(\frac{323}{298} \right) = 4.4958$ LPM

$$\text{linear velocity } u = Q/A = \frac{4495.8}{60} \frac{\text{cm}}{\text{sec.}}$$

$$\frac{\pi}{4} \times (5.27)^2$$

$$= \frac{5.27 \times 4495.8}{60 \times \frac{\pi}{4} \times (5.27)^2 \times 7.780 \times 10^{-6} \times 323^{1.75}}$$

$$U_{av.} = \frac{Q}{\pi (0.2R)^2} = \int_0^{0.2R} \frac{2U [1 - (\frac{r}{R})^2] 2\pi r dr}{\pi (0.2R)^2} = 1.96 U$$

$$\begin{aligned} \text{Reynolds number around the cylinder } Re_D &= \frac{1.96}{4} \times Re_p \\ &= 0.49 \cdot Re_p \\ &= 0.49 \times 94.601 \\ &= 46.04. \end{aligned}$$

In the stagnation region of a circular cylinder we have shown

$$\frac{1}{2} \frac{Sh_D}{\sqrt{Re_D}} = F(Sc) \dots \text{(equation 3.1.29)}$$

where Sh_D is the Sherwood number for mass transfer

Sc is the Schmidt number = 0.20

$Re_D = 46.04$. For $Sc = 0.20$ $F(Sc) = 0.3$.

$$Sh_D = 0.6 \times \sqrt{46.04} = 4.071.$$

The mass transfer coefficient $k_g = Sh_D \times \frac{D_c}{D}$

where D_c is the diffusion coefficient of hydrogen in air.

(from Appendix 1) = $4.6517 \times 10^{-5} \times T^{1.75}$

D is the diameter of the cylinder.

$$\begin{aligned} k_g &= \frac{4.071 \times 4.6517 \times 10^{-5} \times 323^{1.75}}{1.25} \frac{\text{cm}}{\text{Sec}} \\ &= \frac{4.071 \times 4.6517 \times 10^{-5} \times 323^{1.75}}{1.25} \times \frac{3600}{82.06 \times 323} \\ &= 0.4410 \frac{\text{gm. mole}}{\text{hr. sq. cm. atm.}} \end{aligned}$$

The apparent or observed rate constant $K = 0.3067 \frac{\text{gm. mole}}{\text{hr. sq. cm. atm.}}$

By the additivity relation established in Chapter 7

$$\begin{aligned} \frac{1}{K} &= \frac{1}{k_s} + \frac{1}{k_g} \\ \frac{1}{k_s} &= \frac{1}{K} - \frac{1}{k_g} = 0.9931 \end{aligned}$$

The true rate constant $k_s = 1.0069 \cdot \frac{\text{gm. mole}}{\text{hr. sq. cm. atm.}}$

(3) Estimation of characteristic reaction parameters:

$$(1) \bar{C}_n = \frac{\bar{R}_{\text{chem.}}}{R_{\text{diffusion}}} = \frac{k_s}{k_g}$$

$$(2) \bar{\eta} = (1 + \bar{C}_n)^{-1} = \left(1 + \frac{k_s}{k_g}\right)^{-1} = \frac{k_g}{k_s + k_g} = \frac{k_s}{k_s + k_g}$$

$$(3) \phi = \bar{C}_n \cdot \bar{\eta} = \frac{k_s}{k_g} \times \frac{k_g}{k_s + k_g}$$

$$(4) \frac{E_a}{E} = 1 + \left(\frac{\partial \ln \bar{\eta}}{\partial \ln \bar{C}_n}\right)$$

$$\frac{E_a}{E} = \bar{\eta} \text{ for } n = 1.$$

REFERENCES

- Acrivos, A. and Chambre P.L., *Ind. Eng. Chem.* 49, 1025-1031 (1957).
- Acrivos, A., *Chem. Eng. Sci.*, 13, 57 (1960).
- Acrivos, A., *A.I. Chem. J.*, 6-410 (1960).
- Baron, T. , Manning, W.R. , and Johnstone, H.R. , *Chem. Eng. Progr .* , 48, 125 (1952).
- Bircumshaw, L. L., and Riddiford, A.C. , *Quart. Rev*, London, 6, No.2, 157-185 (1952).
- Blasius, H., in Schlichting H., *Boundary Layer Theory*, 4th Edition, New York, McGraw Hill Book Co., 1960, op. cit. 114.
- Boroskov, G.K. , *J. Chim. Phys.*, 51, 759-68 (1954).
- Brunner, E., *Z. Physik. Chem.*, 47, 56-102 (1904).
- Centnerszwer, M. *Z. Physik. Chem.*, A 141, 297-320 (1929).
- Chambre R. L., and Acrivos, A. *J. Appl. Phys.*, 27, 1322-1328 (1956).
- Damkohlor G. *Z. Electrochem.* 42, 846-862 (1963).
- Evans, H.L., *Int. J. Heat Mass Transfer*, 5, 3537 (1962).
- Fetting, P., *Chem. Ing. Tech.* 34, 834 (1962).
- Frank-Kamenetskii, D.A., 'Diffusion and Heat Exchange in Chemical Kinetics', transl. by N.Thor (Princeton University Press, Princeton, N. J. 1955).
- Ford, F.E. and Perlmutter, D.D. , *A. I. Chem. J.*, 9: 371 (1963).
- Friedlander, S.K. and Litt, M. *Chem. Eng. Sci.*, 7:229(1958).
- Friedlander, S.K. and Litt, M. *Appl. Sci. Res.*, 8a:403 (1959)

- Friedlander, S.K. 'Hydrodynamic Solution Chemistry, Convective Diffusion with Chemical Change in Solution, report on N.S.F. Grant-G, 14448 (1962).
- Gidaspov, D. and Ellington, R.T., A.I.Chem. E. Journal, 10, 707 (1964).
- Gidaspov, D. and Ellington, R.T., A.I.Chem. E. Journal, 10, 714 (1964).
- Gildenblunt, I.A. et al., J. Appl. Chem. U.S.S.R., 33-245 (1960).
- Graham R.R. and Vidauri P.I. and Gully A.J., A. I.Ch.E. Journal 14, No.3. pp.473-479.
- Gupalo, Yu. P. and Ryazantser Yu. S. Chem. Eng. Sci., Vol.27, pp.61-68 (1972).
- Haber, F. 'Thermodynamics of Technical Gas Reactions (Longmans Green and Co., London, 1908) p.252.
- Heymach, G.J. Ph.D. Thesis, Univ. of Pennsylvania (1969).
- Heymann H. Z. Physik. Chem., 81, 204-222 (1913).
- Hencil V. and Mitschka, P. and Beranek. L., Journal of Catalysis. 13, 435-444 (1969).
- Hilsenrath J., et al. 'Tables of Thermodynamic and Transport Properties of Air, Argon, Carbon-di-oxide, carbon monoxide, Hydrogen, nitrogen, oxygen and steam', Pergamon Press, Oxford (1960).
- Horvath, C., et al. Chem. Eng. Sci., 2, 126 (1972)

- Horvath, C., et al., *Ind. Eng. Chem. Fund.* 12, 421 (1975).
- Hoelscher, H.E. *Chem. Eng. Prog. Symp. Ser.* 50,
45-50 (1954).
- Hougen, O.A. *Ind. Eng. Chem.* Vol. 53, 509-528 (1961).
- Ibl, N. *Chem. Ing. Tech.*, 35, 353-361 (1965).
- Katz, S., *Chemical Eng. Sci.*, 10, 202 (1959).
- Korenkov, A.I., et al., *Theoretical Foundations of Chem. Engg.* Vol.10, No.4, p. 487 (1976).
- Kulacki, F.A. and Gidasпов, D. *The Canadian Journal of Chemical Engineering* Vol.45, 72-78 (1967).
- Leder F. and Butt J. B., *A.I.Ch.E.J.*, 12(4), 718-21 (1966).
- Levich, V.G., ' *Physicochemical Hydrodynamics* ' (Prentice Hall, Inc. Englewoodcliffs, N.Y., 1962), 2nd Ed.
- Levich V.G., *Acta Physicochim URSS.* 17-257-507 (1942).
- Levich, V.G., *Zu. Fiz. Khim.* 18, 335-355 (1944).
- Levich, V.G., *Discussions Faraday Soc*, 1, 37-43 (1947).
- Levich, V.G. and Meiman, N.N. *Dokl. Akad. Nauk SSSR*,
70, 97-100 (1951); also *Chem. Abstracts* 46.
48922 (1952).
- Lit M. and Friedlander S.K, *A.I. Chem. Journal*, 5,
483 (1959).
- Mashelkar R.A. and Ramachandran P.A. *J. Appl. Chem. Bio technol.* 25, 867-880 (1975).
- Mickley, H.S., Ross, R.C., Squayers, A.L. and Stewart W.E.,
*N.A.C.A. T.N.*3208 (1954).

- Marrco, T.R. and Mason, E.A. J. Phy. Chem. Ref. data,
Vol.1, No.1, p.3 (1972).
- Nornst, W. Z. Physik. Chem., 47-52-55 (1904).
- Nernst, W. and Merriam, E.S., Z. Physik. Chem., 53,
235-244 (1905).
- Newman, A.B. Trans. Am. Chem., Engrs, 27,
203-220 (1931).
- Noyes, A.A. and Whitney, W.R. Z. Physik-Chem., 23,
689-692 (1897).
- Paneth, F.A. and Hertzfeld, K.F. Z. Electrochem.
37, 577 (1931).
- Pignet and Schmidt, L.D. Chem. Eng. Sci. 29, 1123-31 (1974).
- Prandtl, L, in Schlichting H. 'Boundary Layer Theory '
transln. by J.Kestin (Pergamon Press, London,
1955), English Ed.
- Predroditeler, A.S., Zh. Tekhn. Fcz. 11, 893 (1941).
- Predroditeler, A.S., Maskra, Adad. Nauk. SSSR (1949).
- Reid, R.C., and Sherwood, T.K. 'The properties of gases
and liquids. Their estimation and correlation'
II Ed, (1966), McGraw Hill Publications, p.86.
- Rosner, D.E. A. I. Chem. J. 9.321 (1963).
- Rosner, D.E., Chem. Eng. Sci. 19, 1 (1967).
- Satterfield, C.N. and Yeung, R.S.C. Ind. Eng. Chem.,
Fundamentals, 2, 257 (1963).
- Satterfield, C.N. 'Mass Transfer in Heterogeneous
Catalysis', M.I.T.Press, 1970.

- Schlichting, H., 'Boundary layer Theory' 6th Ed. , McGraw Hill Book Co., New York, 1968.
- Schmidt, H. J. Chem. Ing. Tech., 12, 841 (1952).
- Serad, G. Ph.D. Thesis Univ. of Pennsylvania, 1964.
- Silverstein, R.M. and Bassler, R.C. 'Spectrometric Identification of Organic Compounds, 2nd Ed. 1963.
- Spalding, D. B. 'Convective Mass Transfer', Edward Arnold (Publishers) Ltd., London, 1963.
- Sparrow, E.M. , Hallman, T.M. and Siegel, R. Appl. Sci. Res. A 7, 37-52 (1957).
- Thiele, E.W. Ind. Eng. Chem., 31, 916-920 (1939).
- Van Name, R.G. and Hill D.V. Am. J. Sci., 42. 301-332 (1916), also Am. J. Sci. 36, 543 (1913).
- Vielstich, W. Z. Electrochem., 57, 646-655 (1953).
- White, D.E. Ph.D. thesis Univ. of Pennsylvania, 1972.
- Wissler, E.H. and Schechter, R.S. Chemical Eng. Sci., 17, 937 (1962).
- Wheeler, A. 'Reaction rates and Selectivity in Catalyst Pores' Advances in Catalysis (Academic Press, New York (1951), Vol. 3 pp.250-327.
- Zeldovich, J.B., Zh.Fiz. Khim. SSSR 13, 163 (1939).

NOMENCLATURE

A	Absorbance or optical density	(dimensionless)
A_c	Area of the coated surface	(cm^2)
C	Concentration in fluid phase	(gm.mole. cm^{-3})
C_1	Surface concentration of the fluid	(gm.mole. cm^{-3})
C_0	Bulk concentration of the fluid	(gm.mole. cm^{-3})
C_n	The catalytic parameter for n^{th} order surface reaction	(dimensionless)
d	Cell path	(cm.)
D	Diameter of the cylinder	(cm.)
D_c	Diffusion coefficient	($\text{cm}^2 \cdot \text{sec.}^{-1}$)
E	True activation energy	(Cal. gm. mole $^{-1}$)
E_a	Apparent activation energy	(Cal.gm.mole $^{-1}$)
$F(Sc)$	Junction of Schmidt number	(dimensionless)
H()	Function defined by equation (3.2.6)	
j	Rate of mass transfer	(mole. hr $^{-1}$)
k	Boltzmann constant	
K_g	Mass transfer coefficient	($\text{gm.mole.hr}^{-1} \text{ cm}^{-2} \text{ atm}^{-1}$)
K_s	True or intrinsic reaction rate constant	($\text{gm.mole.hr}^{-1} \text{ cm}^{-2} \text{ atm}^{-1}$)
K	Apparent or observed reaction rate constant	($\text{gm.mole.hr}^{-1} \text{ cm}^{-2} \text{ atm}^{-1}$)
L	Characteristic length or length of catalyst plate	(cm.)
m	Function defined by equation (3.1.15)	

M_1, M_2	Molecular weights of the species	(gm.mole ⁻¹)
n	Reaction order	
P	Total pressure	(atms. or mm.Hg.)
P_c	Critical pressure	(atms. or mm.Hg.)
P_v	Vapour pressure	(atms. or mm.Hg.)
R	Universal gas constant	(lit. atm.gm. mole ⁻¹ °K ⁻¹)
Re	Reynolds number, $\frac{DU_\infty}{\nu}$	(dimensionless)
R	Overall rate of reaction	(mole.hr ⁻¹ cm ⁻³)
S	Wetted area of the catalyst	(cm ²)
Sc	Schmidt number, ν/D_c	(dimensionless)
Sh	Sherwood number $\frac{k_g D}{D_c}$	(dimensionless)
t	Time	(minutes)
T	Absolute temperature	(°K)
u	Velocity in the x direction	(cm. sec. ⁻¹)
U(x)	Velocity in the potential flow	(cm. sec. ⁻¹)
U	Velocity in the mainstream	(cm.sec. ⁻¹)
v	Velocity in the y direction	(cm.sec. ⁻¹)
x	Axial coordinate	
y	Transverse coordinate	

Greek letters

α	Defined in equation (3.1.10)
β	Defined in equation (3.1.10)
δ	Boundary layer thickness (cms.)
$\bar{\eta}$	The integrated diffusion (effectiveness) factor (dimensionless)
θ	Dimensionless concentration defined by equation (3.1.25)
λ	Velocity boundary layer defined by equation (3.2.3)
μ	Dynamic viscosity of the fluid ($\text{gm.cm}^{-1} \text{sec}^{-1}$)
ν	Kinematic viscosity of the fluid ($\text{cm}^2.\text{sec}^{-1}$)
ε	Force constant
ω	Defined in equation (3.3.20)
ξ	Defined in equation (3.1.6)
Σ	Defined in equation (3.3.20)
ρ	Density of the fluid (gm. cm^{-3})
σ	Force constant
ϕ	Angle around the cylinder measured from the stagnation region (degrees)
$\bar{\phi}$	Global correction for finite catalyst activity (dimensionless)
ψ	Stream function defined in equation (3.1.5)

Subscripts

av	Average
c	Concentration
Chem	Chemical control
diff	Diffusion control
D	Diameter
0	In the bulk
p	At the pipe
s	At the surface
v	Velocity
x	Local value based on characteristic length
	At upstream infinity